Title: Geometry mismatch and reticular chemistry: strategies to assemble metal-organic frameworks with non-default topologies

Authors: Vincent Guillerm†* and Daniel Maspoch†‡*

Affiliations: † Catalan Institute of Nanoscience and Nanotechnology (ICN2), CSIC and The Barcelona Institute of Science and Technology, Campus UAB, Bellaterra, 08193 Barcelona, Spain; ‡ICREA, Pg. Lluís Companys 23, 08010 Barcelona, Spain

Keywords: metal-organic frameworks, reticular chemistry, rational design, geometry mismatch, self-assembly, porous materials.

TOC image:

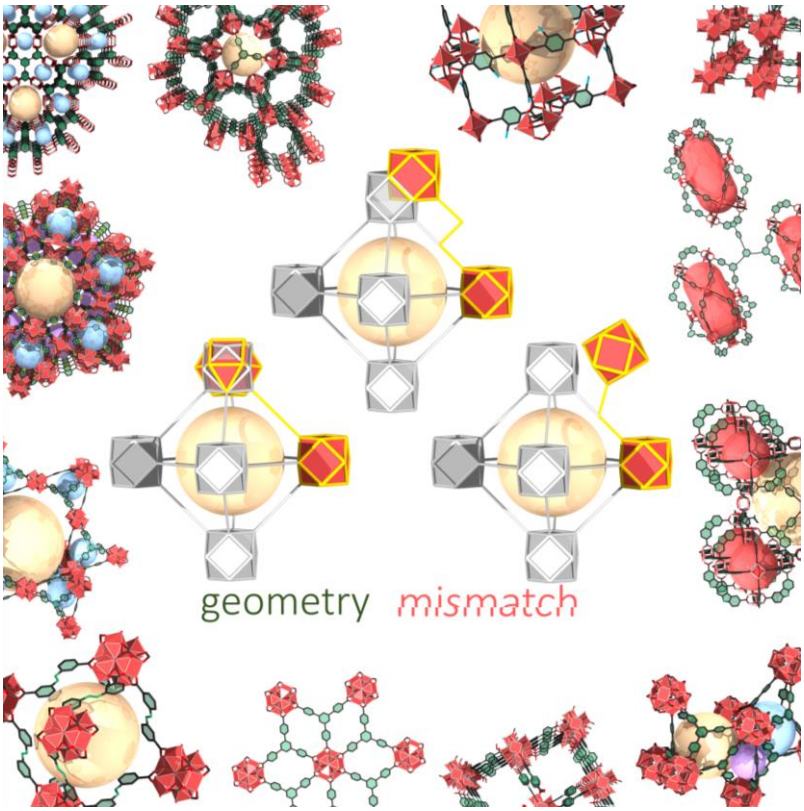

ABSTRACT

The past 20 years have witnessed tremendous advances in the field of porous materials, including the development of novel metal-organic frameworks (MOFs) that show great potential for practical applications aimed at addressing global environmental and industrial challenges. A critical tool enabling this progress has been *reticular chemistry*, through which researchers can design materials that exhibit highly regular (*i.e.* edge-transitive) topologies, based on the assembly of geometrically-matched building blocks into specific nets. However, innovation sometimes demands that researchers steer away from default topologies to instead pursue unusual geometries. In this perspective, we cover this aspect and introduce the concept of *geometry mismatch*, in which seemingly incompatible building blocks are combined to generate non-default structures. We describe diverse MOF assemblies built through geometry mismatch generated by use of ligand bend-angles, twisted functional groups, zigzag ligands and other elements, focusing on carboxylate-based MOFs combined with common inorganic clusters. We aim to provide a fresh perspective on rational design of MOFs and to help readers understand the countless options now available to achieve greater structural complexity in MOFs.

1. Introduction

Since the discovery of MOF-5[1] and HKUST-1[2] some 20 years ago, great efforts have been dedicated to understanding the basic principles that govern MOF assembly.[3] The final structure of a given MOF is now widely understood to be strongly influenced by the geometries of its constituent organic ligands and inorganic moieties (*e.g.* single metal ions, polynuclear clusters, infinite chains, *etc.*). Numerous design approaches such as use of molecular building blocks (MBBs) or secondary building units (SBUs) [4-10] have been combined with the mathematic discipline of topology[11-13] to synthesize myriad novel porous structures,[14] including MOFs that exhibit high performance in crucial environmental and industrial applications such as energy/gas storage separation,[15-18] waste/valuables removal,[19-20] water harvesting[21-25] and smart materials.[26-28]

Concerted efforts by chemists and materials scientists have given rise to a new subfield of chemistry: *reticular chemistry*. The dedicated Reticular Chemistry Structure Resource (RCSR) database created in 2008 by O'Keeffe, Yaghi and coworkers now contains roughly 3,000 three-periodic nets (topologies)[29] and the ToposPro software has been developed to make topology analysis easily available.[30] One might imagine that there would be a limited number of ways to periodically assemble polygons and polyhedra and that all of these topologies would have already been predicted. Surprisingly, this is not the case, even though there are already almost 100,000 MOF structures reported in the MOF subset of the Cambridge structural database.[31] Indeed, there are near-monthly reports of MOFs that exhibit topologies described as "novel", "previously unknown", "unprecedented" or "unique". For instance, Eddaoudi and coworkers revealed more than 100 novel topologies,[32] based on *merged nets*.[9] However, reticular chemistry is not limited to the discovery of novel 3D periodic nets: in fact, researchers have often discovered MOFs whose constituent clusters have never previously been reported as discrete molecules. Some of these clusters have high connectivity, which is a highly desired asset.[33-36] Indeed, the greater the connectivity within the building blocks, the lower number of possible structures attainable upon assembly and consequently, the lesser the chance of obtaining an undesired structure. For example, squares[37-38] or tetrahedra can assemble into numerous structures (248 zeolitic nets known),[39] whereas triangles and rhombicuboctaedra (**rco**) can only assemble into one net, the **rht** topology.[40] Accordingly, researchers have been seeking MBBs[10, 33, 35, 41-47] or supermolecular building blocks (SBBs)[4, 33, 40, 48-49] of high connectivity, with which to rationally construct MOFs. However, whereas most efforts are focused on joining together compatible building blocks to form MOFs of predicable structures and topologies, an opposite strategy would be to combine apparently incompatible building blocks into structures and topologies, which would provide an opportunity to learn about their behavior and access unprecedented materials.[33] Along these lines, scientists can employ less-symmetric organic ligands, with bend-angles,[35] introduce steric hindrance[50] or use zigzag-shaped ligands (transversal reticular chemistry).[51] These strategies all induce structural irregularity known as *geometry mismatch.*

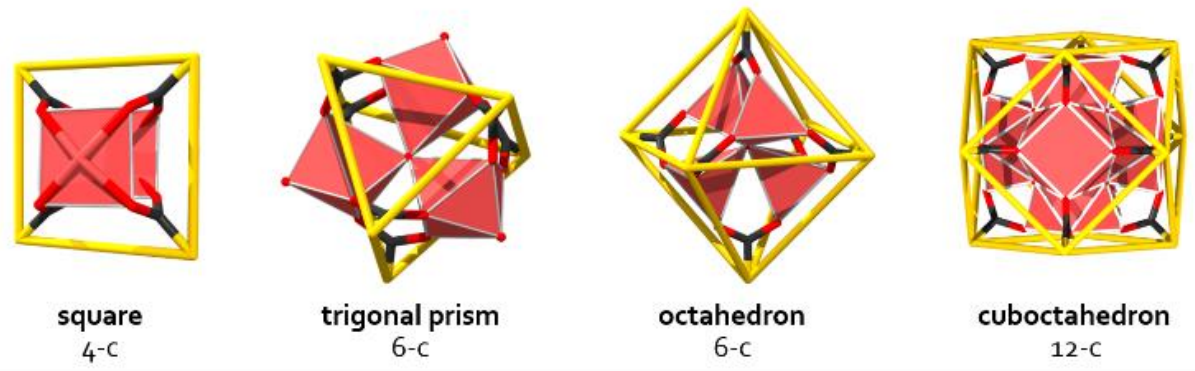

Figure 1. Representation of the four common types of clusters studied in this perspective. Vertex figures matching their points of extension are represented in yellow.

Theoretically, geometry mismatch could be harnessed for any class of MOFs, such as azolate or phosphonate based MOFs. However, in this perspective, we focus on carboxylate-based MOFs combined with common inorganic MBBs (*i.e.* those for which the synthetic conditions are well known). Given their abundance in the Cambridge Structural Database,[52] we consider the following clusters

suitable for reliable analysis: M^{II} *(Cu, Zn, Co, etc.) paddle wheels*, as in HKUST-1;[2] M^{III} *(Fe, Cr, Sc, Ga, Al, etc.) trimers*, as in MIL-100;[53] *Zn tetramers*, as in MOF-5;[1] and $M^{III/IV}$ *(rare earths [RE], Zr and Hf) hexamers*, as in UiO-66 (Figure 1).[54] Thus, here we describe examples of MOFs and synthetic strategies that have pushed the envelope of reticular chemistry, challenged standard assembly rules and enabled high degrees of structural complexity, all thanks to the geometry mismatch generated through assembly of their (apparently incompatible) respective building blocks.

2. Topological tools in reticular chemistry: a precious but limited asset

2.1. Nets, nodes, augmented nets and vertex figures

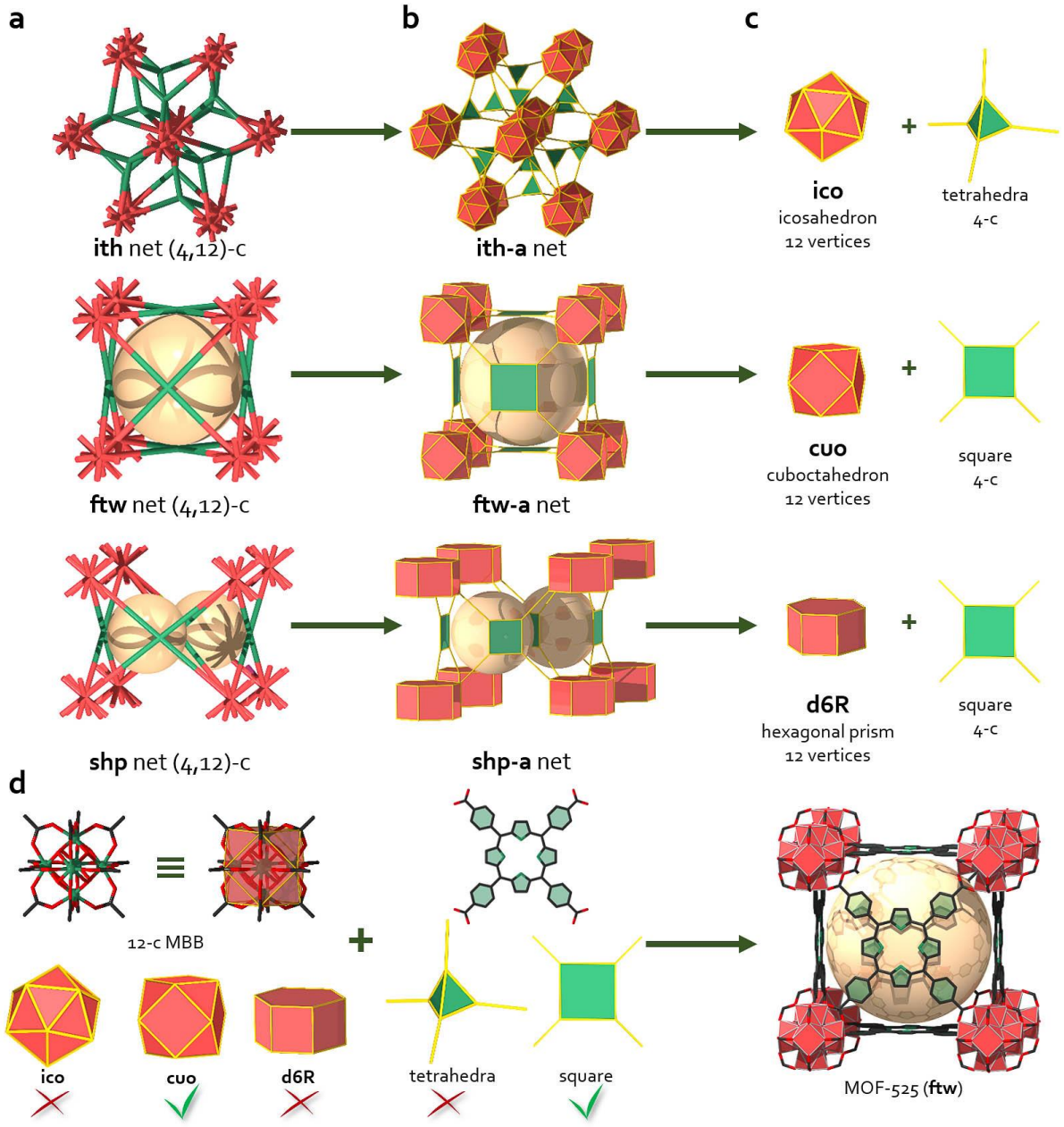

Figure 2. a) The three edge-transitive (4,12)-c nets **ith**, **ftw** and **shp**. b) Augmented representation of the three edge-transitive (4,12)-nets **ith-a**, **ftw-a** and **shp-a**. c) Polygonal and polyhedral building units resulting from the deconstruction of augmented nets. d) Topology prediction map for the assembly of a 12-c hexanuclear cluster with 4-c tcpp ligand, leading to the **ftw**-type structure of MOF-525.

In this section, we briefly highlight the role of topology in the standard design strategy for MOF synthesis, endeavoring to help novices understand the potential and limits of topology in structure design and prediction, through the relatively counterintuitive strategies that we describe in this perspective. In fact, reticular chemistry has always been associated with topology, and several articles from Delgado-Friedrich *et al.* have been a major source of inspiration for molecular architects.[11-12, 55-58] Targeting a specific MOF requires selection of at least one organic MBB and one inorganic MBB, each of which will have a specific connectivity (*i.e.* the number of other MBBs it will be linked to). Ideally, assembly of these building blocks would be limited to only one possible structure. The resultant three-periodic net should be as regular as possible, preferably edge-transitive (*i.e.* having only one type of edge bridging the nodes of the net), such that the risk of obtaining undesired structures is minimized.

As an illustrative example, we consider the ideally 12-connected (12-c) Zr hexanuclear cluster and the 4-c ligand, tetrakis(4-carboxyphenyl)porphyrin (tcpp). The expected topology would be an edge-transitive (4,12)-c net. According to the RCSR database, three such nets exist: **ith**, **ftw** and **shp** (Figure 1a). To differentiate among these three nets and find the expected topology, one must inspect the corresponding augmented nets (**net-a,** Figure 1b), in which the vertices (nodes) are replaced with the corresponding vertex figures (polygons or polyhedra). Such inspection reveals that **ith**, **ftw** and **shp** differ from each other: thus, **ith-a** is the combination of icosahedra with tetrahedra; **ftw-a** comprises cuboctahedra linked by squares; and **shp-a** comprises hexagonal prisms and squares (Figure 1c). In parallel, the twelve extension points of the Zr cluster together form a cuboctahedron, whereas the four extension points of the tcpp ligand form a square. Therefore, formation of the nets **ith** or **shp** can be excluded. Consequently, for a MOF with 12-c Zr cluster and a 4-c tcpp ligand, the expected topology is **ftw** (MOF-525, Figure 1d).[59]

2.2. Angles, offset and twists in organic ligands: limitations of topology in MOF design

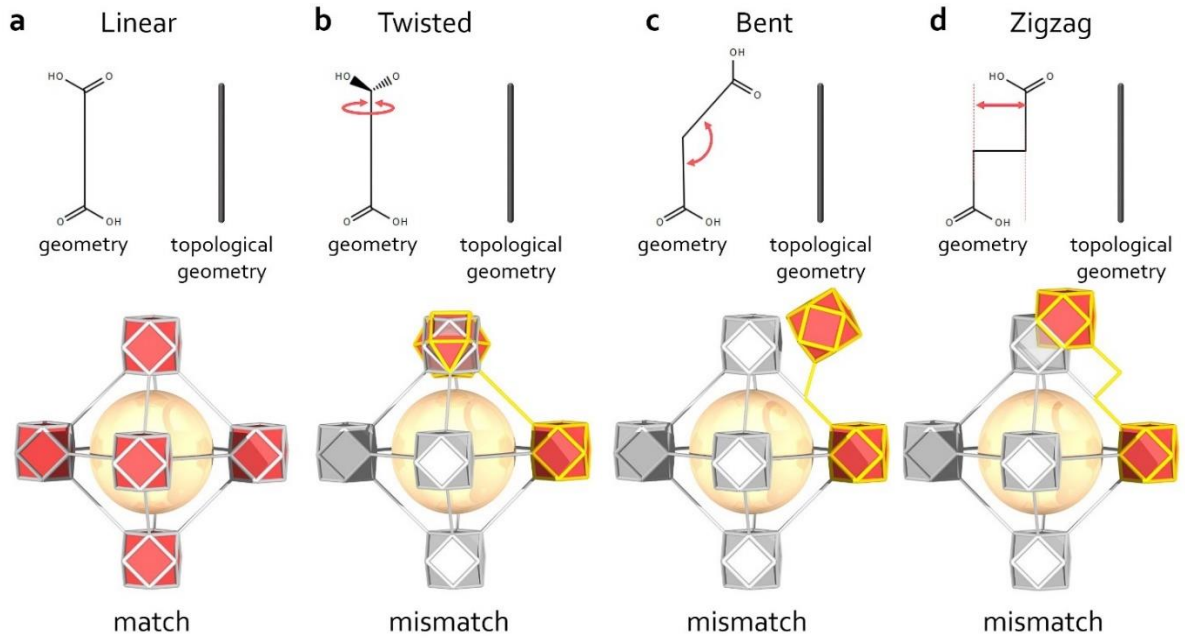

Figure 3. Schematic representation of a) the **fcu-a** net and how b) twisted, c) bent or d) zigzag ligands would create geometry mismatch.

After illustrating the prime importance and power of topology as a design tool in reticular chemistry, we address here its relative weakness. Indeed, the simplification of a structure into its underlying net (topology) reduces MBBs as nodes, or for the case of ligands that are 2-connected, it is simply discarded and corresponds to the edges of the net. For instance, UiO-66 comprises 12-c Zr MBBs bridged by 2-c terephthalates; however, the corresponding **fcu** topology is uninodal (12-c net). Therefore, it is difficult

to gain insight *a priori* on the possible effects of different ligand geometries (*i.e.* introducing a twist, an angle or an offset into a 2-c ligand) on the resulting structure or topology, apart from evidence that it might create geometry mismatch and thus, prevent formation of the default structure or topology (Figure 3). In the following sections, we aim to elucidate existing strategies and remaining challenges for the efficient design of MOFs with less regular, non-default topologies.

3. Ditopic ligands

3.1. Linear, twisted ligands with steric hindrance: a cornerstone of MOF design

*In this section, the default topologies are the edge-transitive **sql** net (4-c), in the case of 4-c paddle wheels, and **fcu** net (12-c), in the case of Zr/Hf/RE hexanuclear clusters ("UiO type cluster"). Both types of MOFs assemble by bridging linear ligands with coplanar carboxylate groups. Breaking this coplanarity by introducing steric hindrance creates geometry mismatch (Figure 3b).*

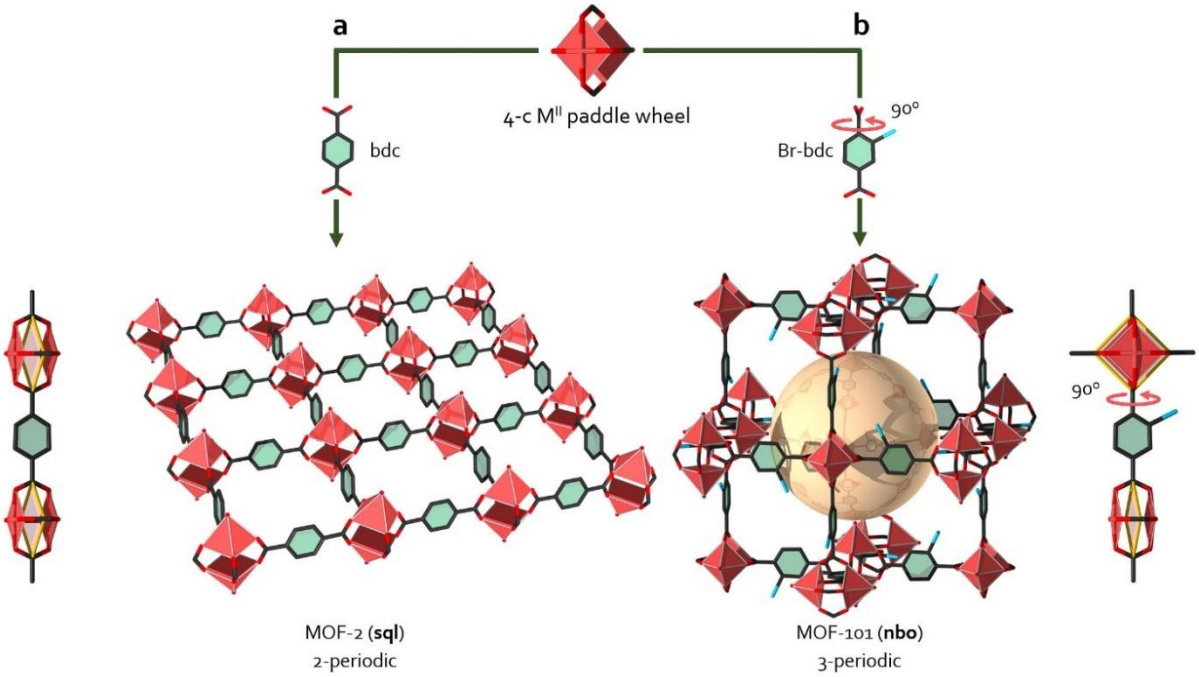

Figure 4. Assembly of bdc or Br-bdc with paddle wheels leads to a) 2-periodic (MOF-2, **sql**) or b) 3-periodic (MOF-101, **nbo**) structures, respectively.

Until 2002, the majority of reported structures resulted from either isoreticular expansion of known MOFs, to create isoreticular MOFs (IRMOFs),[60] or from exploratory trial-and-error work.[2, 61-65] Then, the report of MOF-101, a Cu dicarboxylate, appeared as a cornerstone of rational MOF design in reticular chemistry (Figure 4).[50] To modify the orientation of the Cu paddle wheels, the coplanarity between the two carboxylic groups in the linear terephthalate (bdc) was broken, by employing a sterically hindered ligand (Br-bdc). This altered the directionality of the connectivity points by 90º, enabling formation of a 3-periodic structure with the **nbo** topology (Figure 4b), rather than the **sql** topology of MOF-2 (Figure 4a).[64] However, the twist angle does not need to be as large as 90º to affect the structure and topology of a MOF. For example, smaller twists in the ligands (28º and 47º) will alter the directionality of the paddle wheels to a lesser extent than in MOF-101. Using this approach, Furukawa *et al.* formed MOF-604, which exhibits the **cds** topology.[37] This strategy has also been applied with longer ligands such as 2,2′-dimethyl biphenyl-4,4′-dicarboxylate (Me_2bpdc)[37] as well as with zirconium, enabling formation of Zr-based MOFs with the **bcu** topology,[66-68] rather than the **fcu** topology, which is commonly obtained when linear ligands are used.[41, 54, 69-72] Lü *et al.* described a surprising example along these lines, having assembled the complex, chiral N,N′-di-(4-benzate)-1,2,6,7-tetrachloroperylene-3,4,9,10-tetracarboxylic acid diimide (pdi) with zirconium. [73] The dihedral angle

between the two carboxylates (38°), and the unusual length and slight flexibility of the ligand, together generated the **dia** topology, rather than the **fcu** or **bcu** topologies. In this structure, the Zr clusters of Zr-PDI are capped by eight ligands, such that each cluster is connected to four others (*i.e.* two ligands each bridge two similar clusters). As a concluding example, we consider the zinc tetramer used to produce IRMOFs.[60] Interestingly, unlike in the case of M^{II} paddle wheels (Figure 5a) and $M^{III/IV}$ hexanuclear clusters (Figure 5c), for IRMOFs, introducing a 90º twist into the organic ligands does not have any impact on the resulting connectivity directions of the cluster (Figure 5b). This is due to the octahedral connectivity of the zinc tetramer. To the best of our knowledge, this observation has not been reported elsewhere.

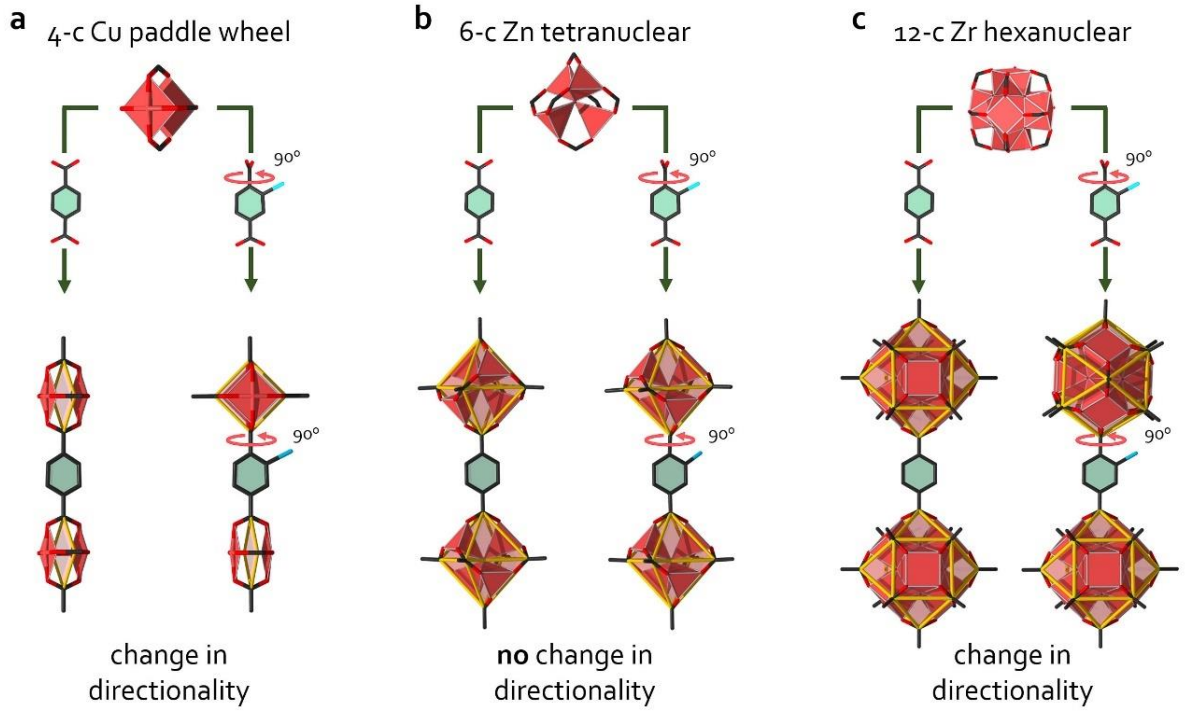

Figure 5. Comparison of the ideal orientation and directionality of MBBs with coplanar or 90º-twisted dicarboxylate ligands. Upon a 90º twist, Cu paddle wheels (a) and Zr hexamers (c) undergo a change in directionality, whereas Zn tetramer (b) maintain their directionality.

3.2. Bent ligands: the door to polymorphism

*In this section, the default topologies are the edge-transitive **sql** net (4-c), in the case of 4-c paddle wheels, and **fcu** net (12-c), in the case of Zr/Hf hexanuclear clusters ("UiO type cluster"). Both types of MOFs assemble by bridging linear ligands with coplanar carboxylate groups. Breaking this linearity by introducing a bending angle (Figure 3c), through use of a bent ligand, creates geometry mismatch; consequently, the ligands that surround the same MBB end up having many distinct orientations.*

Combining paddle wheels with bent ligands of various angles leads mainly to discrete metal-organic polyhedra (MOPs) molecules [74-75] and to 2D MOFs (**sql** and **kgm**).[38] For MOPs generated with square building units (paddle wheels or single metal ion), the influence of the bend-angle in the ligand is clear, enabling isolation of MOPs of various geometries and distinct organic/inorganic content (*i.e.* metal/ligand [M/L] content), which has already been well documented elsewhere.[4, 76-81] To illustrate the influence of bent ligands on MOF assembly, we have chosen hexanuclear Zr/Hf clusters as the representative inorganic MBB (Figure 6), owing to their usually high and adaptable connectivity (from 4 to 12). Introducing an angle into a dicarboxylic ligand (*i.e.* changing the directionality of its connectivity) can, depending on the bending angle, prevent the formation of the ubiquitous **fcu**-type framework (Figure 3c). Interestingly, at an angle of 160º, such as that in the ligand 9-fluoreneone-2,7dicarboxylate (fldc), found in BUT-10, the topology remains **fcu** (Figure 6a).

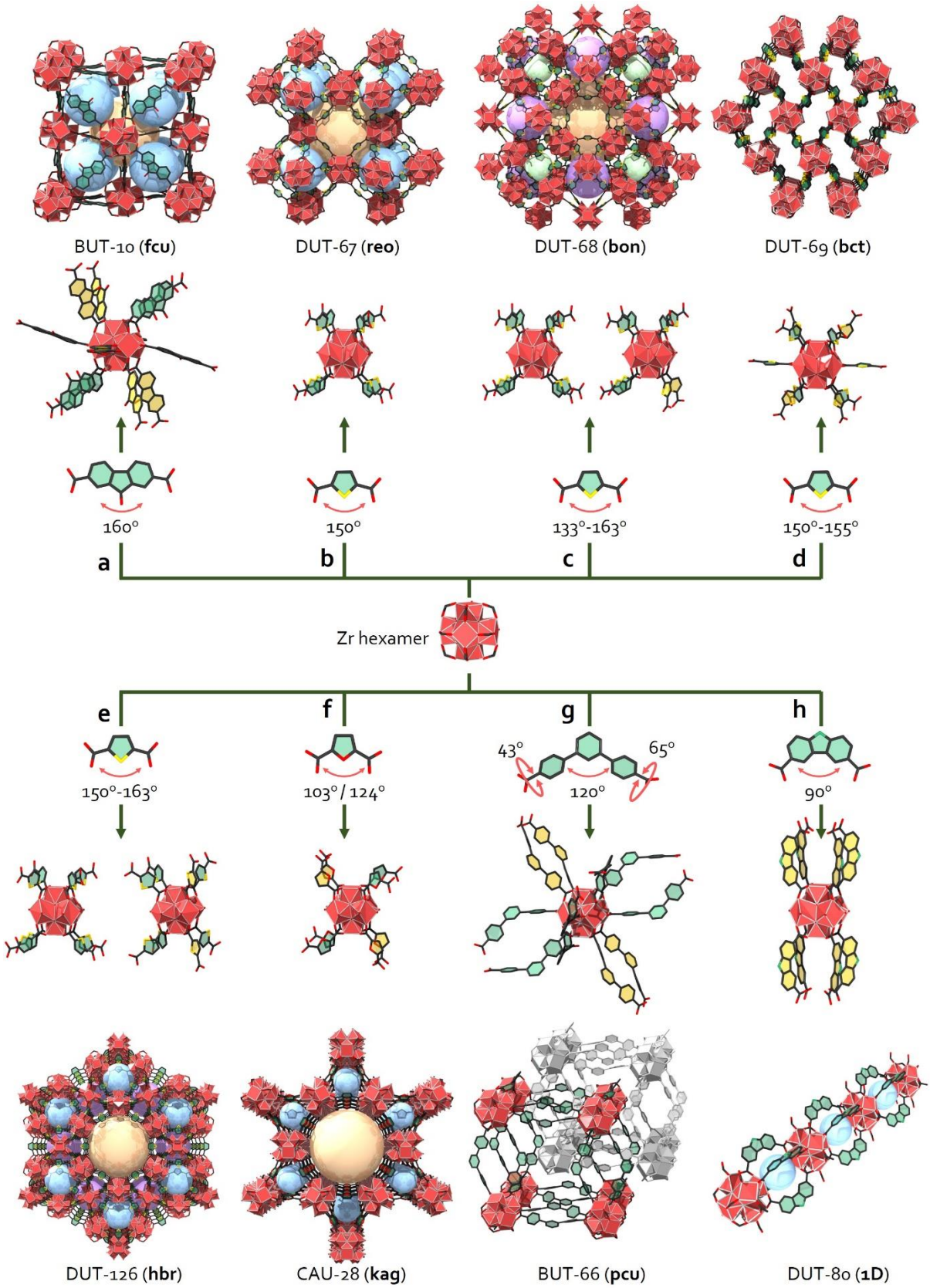

Figure 6. Varying the angle, and/or the orientation around Zr based clusters, of bent ligands leads to MOFs with a) the **fcu** (BUT-10), b) **reo** (DUT-67), c) **bon** (DUT-68), d) **bct** (DUT-69), e) **hbr** (DUT-126), f) **kag** (CAU-28) or g) **pcu** (BUT-66) topologies, as well as to 1D coordination polymers (DUT-80). Some organic rings are filled in yellow to better distinguish the ligand orientations around the clusters.

However, to offset the effects of the bend-angle, the clusters exhibit an overall inclination of *ca.* 14º from their ideal orientation.[82] At smaller angles, such as *ca.* 150º, as in the case of the ligands dithienothiophene dicarboxylate (dttdc) and 4,4'-(2 H-1,2,4-triazole-3,5-diyl) dibenzoate (tadiba), the angle has a large influence on the outcome, leading to the **reo**-MOFs DUT-51[83] and JLU-MOF58,[84] respectively. Interestingly, using a shorter ligand of comparable angle, 2,5-thiophenedicarboxylate (tdc), leads to four distinct structures: three 8-c nets (the **reo**-MOF DUT-67[85] [Figure 6b] and its two polymorphs, the **bon**-MOF DUT-68 [Figure 6c][85] and the **hbr**-MOF DUT-126 [Figure 6e][86]), and one 10-c net (the **bct**-MOF DUT-69 [Figure 6d][85]), whose rare topology is also found in MOF-802, which is based on the ligand 3,5-pyrazoledicarboxylate (pzdc).[25] These examples highlight the great potential of bent ligands to promote structural diversity, by conferring the bent ligands around the Zr clusters with different orientations without necessarily altering the connectivity of the binding groups (Figure 6). An intriguing case is CAU-28 (Figure 6f),[87] which comprises two crystallographically distinct 2,5-furane dicarboxylate (fdc) ligands, one of which exhibits a 124º angle, four of them surrounding the Zr/Ce clusters and bridging them into a Kagomé lattice. The other ligands (four per cluster), which have a markedly smaller angle (*ca.* 103º), act as "pillars" between the layers along the *z* axis, to form an overall **kag** topology.

No section on bend-angles would be complete without mentioning a bent ligand with a 120º angle. Surprisingly, and to the best of our knowledge, no one has yet reported assembly of a MOF from Zr clusters and the ubiquitous 120º bent isophthalate ligand (*m*-bdc). However, Xie *et al.* did recently report combination of Zr clusters with either 4,4'-(benzene-1,3-diyl)dibenzoate (bdb) or 4,4'-(naphthalene-2,7-diyl)dibenzoate (ndb) to form the **pcu**-MOFs BUT-66 (Figure 6g) or BUT-67, respectively.[88]

Although their clusters are 12-connected, these MOFs exhibit the same topology as in MOF-5: each Zr cluster is bridged to six others by pairs of ligands. Similarly to Xie *et al.*, Wei *et al.* subsequently reported that combination of Gd hexanuclear clusters and tetrafluoroisophthalate (*m*-bdc-F_4) generates a **pcu**-MOF.[89]

Finally, Krause *et al.* evaluated an even smaller angle, of 90º, in their assembly of a MOF from Zr clusters and the ligand 9h-carbazole-3,6-dicarboxylate (cdc) into the 1D coordination polymer DUT-80 (Figure 6h). In this structure, the 8-c Zr clusters are quadruple-bridged to each other by cdc ligands to form "chains" of clusters, which can be connected together to yield the flexible MOF DUT-98 (*vide infra*).[90]

Overall, the case of MOFs assembly with bent ligands still represents a major challenge in terms of net predictability. The many possibilities of varying angles and the numerous ways of orienting the ligands around the clusters prevents for easy rationalization. We anticipate recent and future advances in computational chemistry will permit a better understanding of these systems in a near future.

3.3. Zigzag ligands: transversal reticular chemistry

*In this section, the default topology is the edge-transitive **fcu** net (12-c) with Zr/Hf hexanuclear clusters ("UiO type cluster"). Such MOFs assemble by bridging linear ligands with coplanar carboxylate groups. Breaking this linearity by introducing a transversal offset creates geometry mismatch (Figure 3d).*

In addition to linear, twisted or bent ligands, another type of ditopic bridge, *zigzag ligands* (Figure 3d), is currently gaining attention in MOF assembly.[91] Examples of MOFs built with such ligands, in which the collinearity between chelating groups is broken, have been reported.[92-94] However, before the advent of transversal reticular chemistry, no clear focus had been made on the potential of their unique shape (Figure 7a).[51] By adding the transversal parameter of width (**w**) to the height (**h**) of the ligands, Guillerm *et al.* demonstrated that, along with making ligands taller or shorter, they could also stretch them transversally, thus breaking the collinearity of the binding carboxylates. In the case of Zr-based MOFs, this effect is reflected by generation of geometry mismatch (Figure 7b), as zigzag ligands do not match the perfect alignment of Zr clusters. Thus, assembling Zr clusters with zigzag ligands leads to **bcu**-MOFs, which can be regarded as **fcu**-MOFs with systematic, ordered defects — namely, four missing ligands on each MBB (Figure 7c).[51] Guillerm *et al.* reported Zr-**bcu**-MOFs (Figure 7e-h) with *trans, trans* muconate (tmuc), 2,6-naphthalene dicarboxylate (26ndc), 2,2'-bipyridine-4 4'-dicarboxylate

(22bipy44dc) or azobenzene-3 3'-dicarboxylate (azo33).[51] Additionally, Maurin, Serre and co-workers used simulations to predict that Zr clusters and zigzag succinate (suc) ligand would combine to form another MOF, Zr-**bcu**-suc (MIP-204, Figure 7d), whose assembly they subsequently confirmed experimentally.[95]

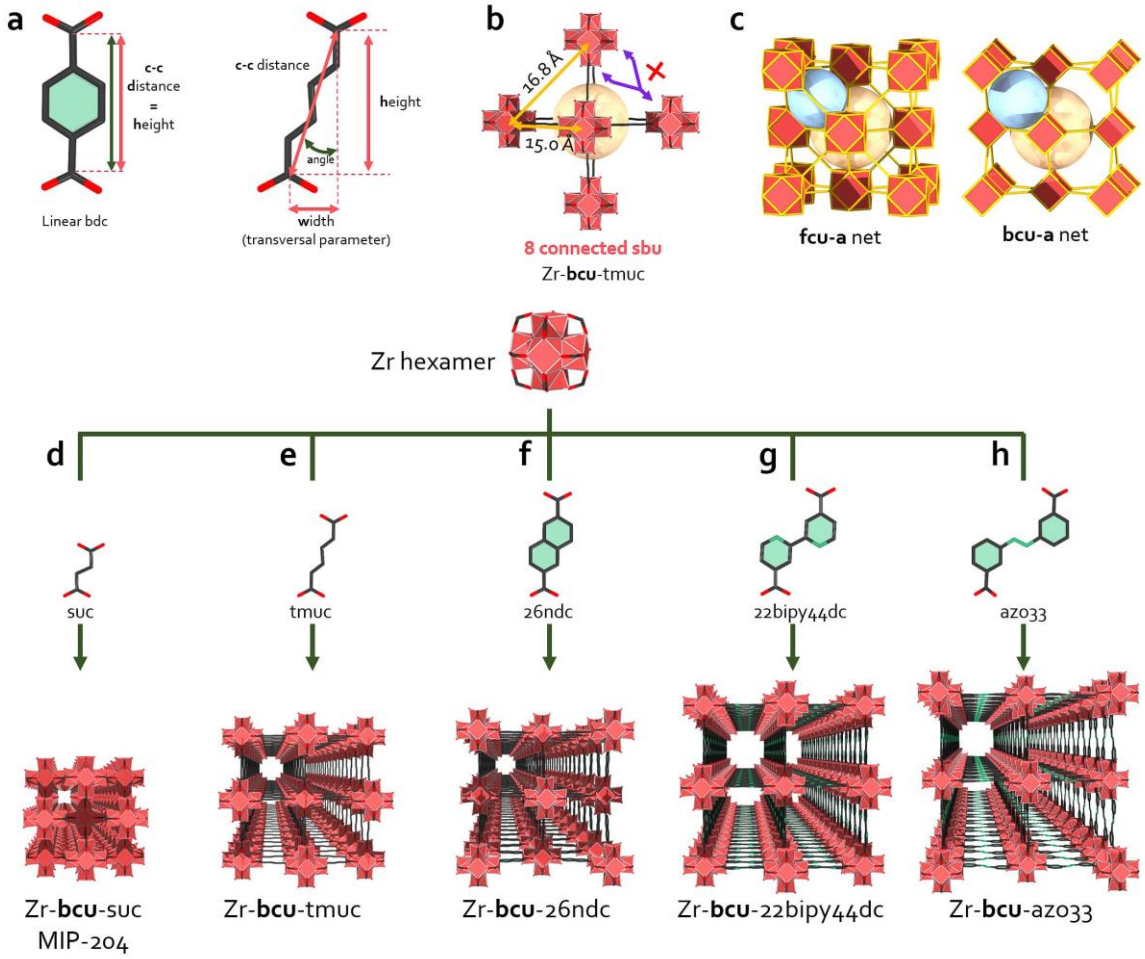

Figure 7. a) Comparison of the characteristic distances and angle in bdc (linear) and tmuc (zigzag) ligands. b) schematic of the geometry mismatch in Zr-**bcu**-tmuc. c) comparison between the **fcu-a** and **bcu-a** nets. A family of isoreticular Zr-**bcu**-MOFs based on d) suc, e) tmuc, f) 26ndc, g) 22bipy44dc or h) azo33 ligands.

Shortly after, by introducing steric hindrance by the mean of a sulfonic group on a 26ndc ligand, Nguyen *et al.* showed the possibility to not only deviate from the 12-c **fcu** net to the 8-c **bcu** net, but also to assemble its polymorphic analog, the 8-c **reo** net.[96]

As in the case of bent ligands, the many possibilities of orienting zigzag ligands around a cluster is a great challenge to tackle in order to achieve rational design of such MOFs. The help of computation tools will surely be crucial to understand and predict the assembly of MOFs with such complex ligands.

The case of ligands with small widths, such as 26ndc and azobenzene-4 4'-dicarboxylate (azo44), is worth mentioning. Some of these act as linear ligands, as their disorder in the framework compensates for their small width values without affecting the cluster orientation or reducing the overall symmetry (Figure 8).[85, 97]

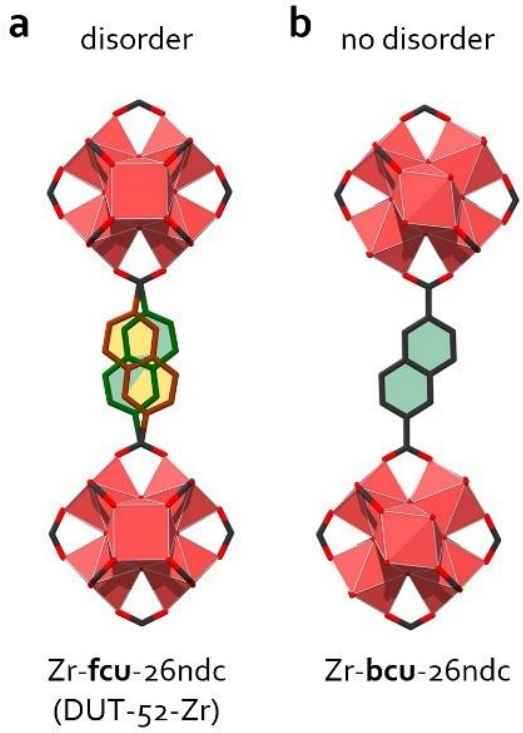

Figure 8. Detail of the 26ndc ligand disordered in Zr-**fcu**-26ndc (DUT-52-Zr) and ordered Zr-**bcu**-26ndc.

Multi-functionality has recently become a highly-desired property for MOFs, as it facilitates their selective post-synthetic modification.[98-99] Many multivariate MOFs have been reported,[9, 100-106] most of which contain randomly distributed ligands having similar shapes but carrying diverse functional groups.[104] Strategies to achieve ordered multi-functionality include ligand insertion/pore partition,[66-67, 107] use of programmed pores[108] and assembly of merged nets.[9] Transversal reticular chemistry is taking crystal engineering to the next level, by enabling selective postsynthetic placement of ligands (*i.e.* functional groups) to create materials that mimic natural structures such as proteins and nucleic acids. For instance, Kim *et al.* reported ready functionalization of the MOF Zr-**bcu**-26ndc (Figure 9a) with tagged terephthalates to produce ordered, multivariate **fcu**-MOFs.[109] To complete the coordination of the Zr clusters in Zr-**bcu**-26ndc assembled through transversal reticular chemistry (*vide supra*), they filled the resultant unoccupied positions with their desired ligand (Figure 9b).

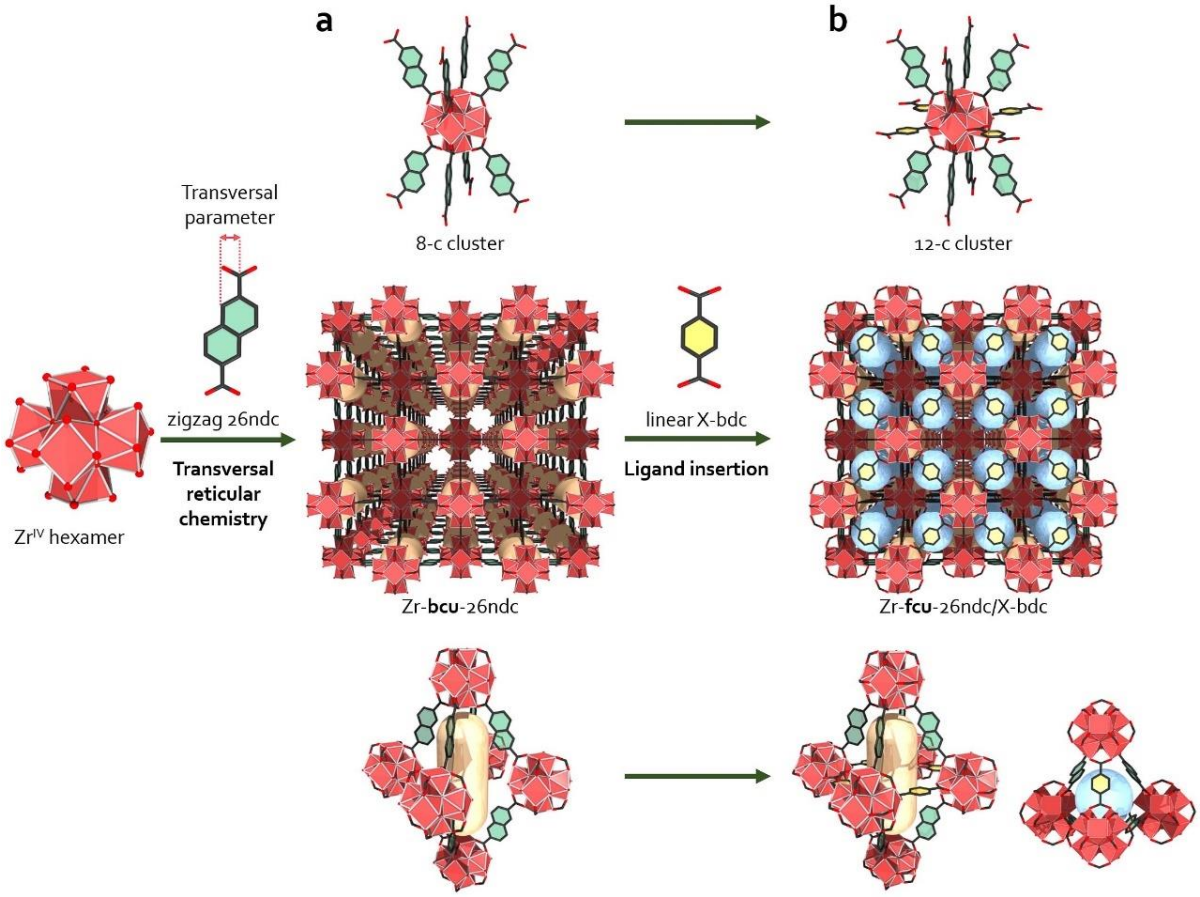

Figure 9. Transversal reticular chemistry enables precise insertion of additional ligands to transform a) Zr-**bcu**-26ndc into b) Zr-**fcu**-26ndc/x-bdc, by completing the coordination of the Zr hexamer (from 8-c to 12-c). Consequently, the channels in Zr-**bcu**-26ndc are transformed into the tetrahedral cages in Zr-**fcu**-26ndc/x-bdc.

Introducing a zigzag ligand into a MOF can influence the MOF's geometry without impacting its overall topology (Figure 10). For example, Chevreau *et al.* described the case of MIL-142B (Figure 10a), an Fe-**nht**-MOF constructed with 4,4'-biphenyldicarboxylate (44bpdc) and 4,4',4'',-benzene-1,3,5-triyl-trisbenzoate (btb),[100] whose framework is interpenetrated, yet whose transversal reticular analog, MOF-909 (Figure 10b), which contains azo33 instead of 44bpdc, comprises a single **nht** net. This is due to the distortion of the framework, preventing intergrowth of a second **nht** net.[110] Interestingly, Nguyen *et al.* reported that introduction of 50% of azo33 is sufficient to prevent its interpenetration (MOF-908).

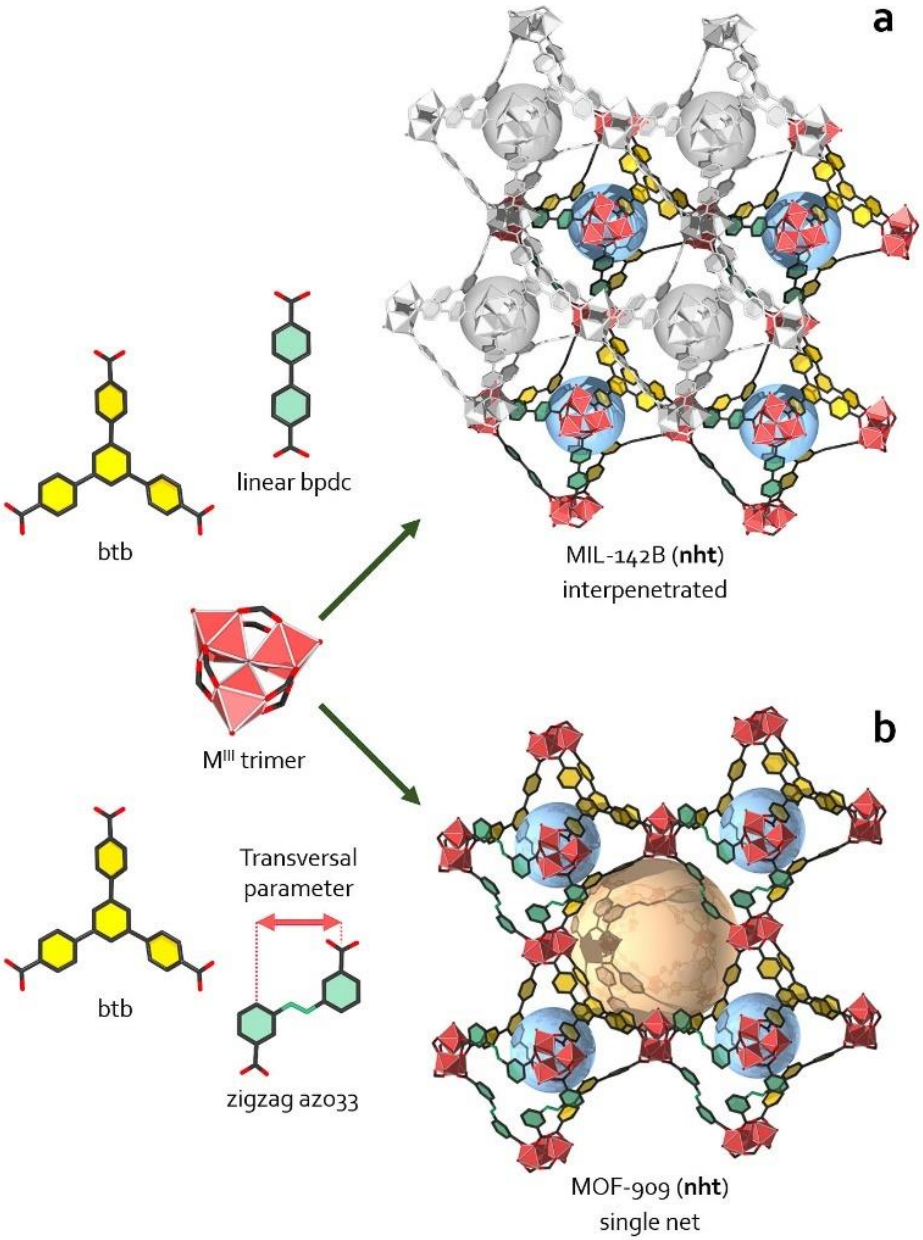

Figure 10. a) In **nht**-MOF MIL-142B, substituting linear 44bpdc with b) zigzag azo33 in MOF-909 prevents interpenetration.

4. Polytopic ligands with various angles and/or twists

4.1. Triangular ligands and cuboctahedral building blocks: geometry mismatch *par excellence*

In this section, there is no edge-transitive net to assemble regular triangles (equilateral, coplanar carboxylates) with 12-c Zr/Hf/RE hexanuclear clusters ("UiO type cluster"). Therefore, all existing structures arise from geometry mismatch, which explains the high variety of topologies (Figure 11).

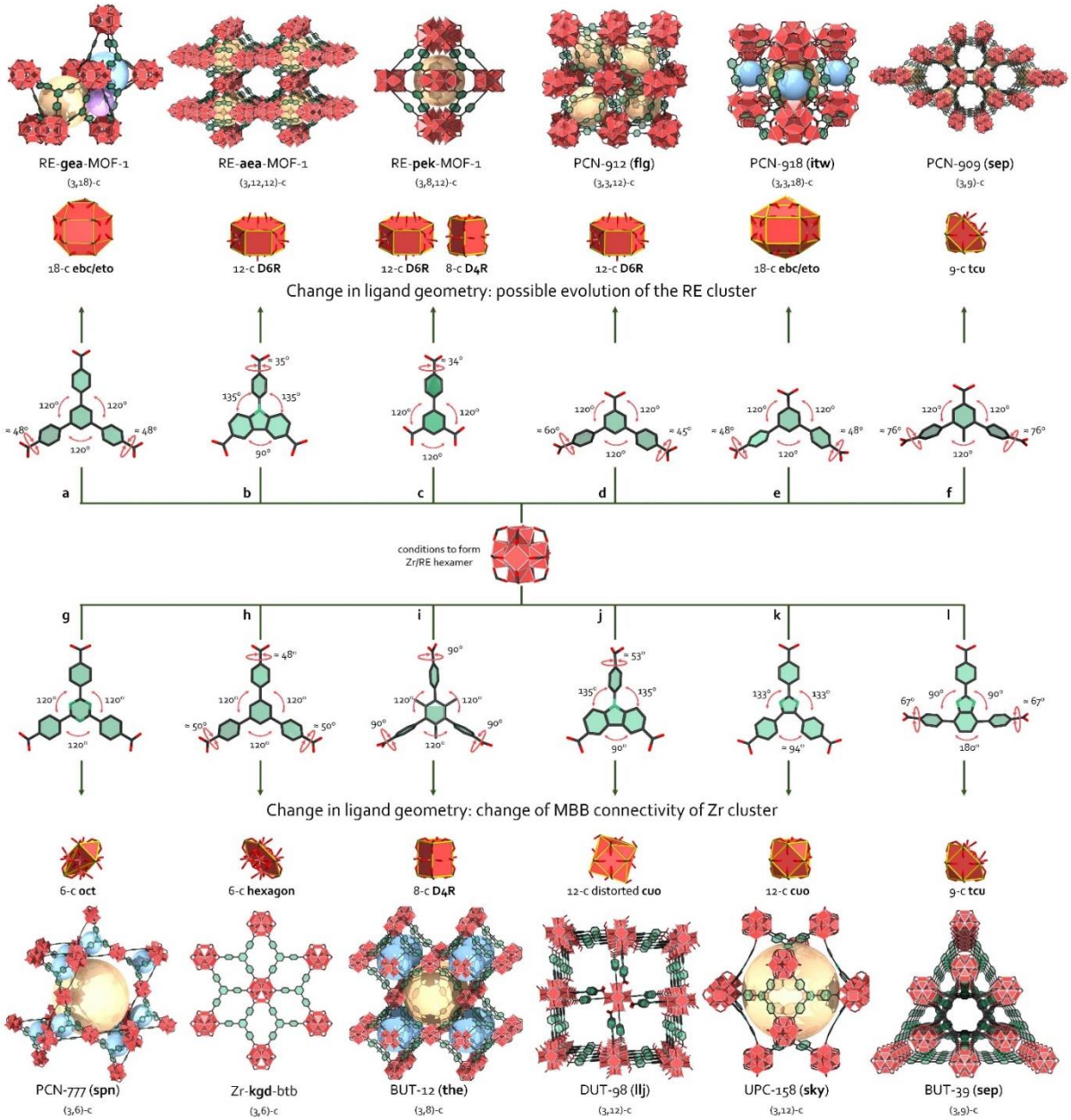

Figure 11. a-f) Summary of the RE-based MOFs and g-l) Zr-based MOFs resulting from assembly of RE/Zr with triangular ligands in the appropriate conditions to form RE/Zr hexanuclear clusters.

4.1.1. The rare earths example

In 2014, upon noticing the apparent incompatibility of 3-c ligands with 12-c (cuboctahedra) clusters (which lacks a corresponding edge-transitive net), Guillerm *et al.* envisioned the possibility of unveiling novel clusters and topologies, which had yet to be discovered in rare-earth and MOF chemistries.[33] After determining the conditions to form the desired rare-earth hexanuclear cluster as a discrete entity, they used similar conditions, in combination with btb. Their system was highly versatile, as additional metal ions and carboxylates caused the hexanuclear cluster to spontaneously evolve into an 18-c, nonanuclear cluster, which was compatible with 3-c btb and gave rise to an unprecedented, minimal transitive, (3,18)-c net with **gea** topology (Figure 11a). Further studies on this net revealed its suitability for rational design of MOFs using supermolecular building blocks (SBBs),[4] which we discuss later in this perspective.[33] Subsequently, Eddaoudi and co-workers also studied the effects of varying the angles of 3-c ligands.[35] Using the 90° angle provided by the ligand 9-(4-carboxyphenyl)-9H-carbazole-3,6-dicarboxylate (bcdc), they were able to unveil yet another nonanuclear cluster, a 12-c one that differs slightly from

that observed in **gea**-MOF-1 (Figure 11a) and which led to formation of a MOF with a novel (3,12,12)-c net, **aea** topology (Figure 11b). In parallel, they demonstrated that reducing two branches of the btb ligands (*e.g.* by using the [1,1'-biphenyl]-3,4',5-tricarboxylate ligand [bptc]) generated another previously unknown topology, **pek**, and that in the resulting **pek**-MOFs (Figure 11c), a 12-c nonanuclear cluster coexisted with the classical hexanuclear cluster (albeit, with connectivity reduced to eight). Finally, by using the extended ligand 5-(4-carboxybenzyloxy)isophthalate (obi), they prepared the isoreticular analog **pek**-MOF-2. Inspired by these reports, Wang *et al.* recently discovered three novel MOFs in the RE/3-c ligand system: PCN-912 (Figure 11d), PCN-918 (Figure 11e) and PCN-909 (Figure 11f). They obtained these MOFs by reducing one branch of the btb ligand and introducing various levels of steric hindrance (using functionalized [1,1':3',1"-terphenyl]-4,4",5'-tricarboxylate ligands [R-tptc]).[44] They unveiled two novel highly-connected nets: the (3,3,12)-c net, **flg** (PCN-912); the (3,3,18)-c net, **ytw** (PCN-918); and also isolated a **sep**-MOF (PCN-909), with the same (3,9)-c net as in the previously reported Zr based MOF, BUT-39 (*vide infra*).[111]

4.1.2. The zirconium example

Under many synthetic conditions, zirconium can produce a similar hexanuclear cluster to that of rare earths (*vide supra*).[112-113] Since the first report of UiO-66 in 2008,[54] and given the success achieved by forcing competition between monotopic acids (as modulators) and polytopic acids in their crystallization,[41, 71-72, 114] Zr-MOFs have become some of the best-studied MOFs.[34, 115-117] These findings paved the way towards construction of MOFs with topologies other than **fcu**. For instance, in 2012, Morris *et al.* described assembly of Zr-MOFs with square ligands. They obtained the expected MOF-525 and MOF-535, which exhibit the edge-transitive **ftw** topology, and surprisingly, also obtained MOF-545, which shows another edge-transitive net, **csq**, whose hexanuclear cluster exhibits a connectivity reduced to eight (the first-ever reported example of this in a MOF).[59]

Regarding equilateral triangular ligands with coplanar carboxylate groups, since they cannot be assembled with 12-connected cuboctahedral shapes, the clusters instead reduce their connectivity to eight, to fit to edge-transitive nets having lower connectivity. This adaptability of the Zr clusters explains the generation of the two **spn**-MOFs MOF-808[25] (ligand: trimesate [btc]) and PCN-777 (ligand: 4,4′,4″-s-Triazine-2,4,6-triyl-tribenzoate [tatb], Figure 11g),[118] whose Zr clusters are six-connected with octahedral directionality. Similarly, Wang *et al.* reported that in presence of btb, Zr clusters also exhibit six-connectivity, albeit in hexagonal directionality, leading to formation of a **kgd**-MOF based on edge-transitive **kgd** layers that interpenetrate to form an overall 3D framework (Figure 11h). In this MOF, the carboxylates are slightly twisted (38º and 46º) relative to the ligand plane.[119] An example of a MOF in which the carboxylates show a greater twist angle (90º) was given by Wang and co-workers, who reported that Zr clusters reacted with 4,4',4''-(2,4,6-trimethyl-benzene-1,3,5-triyl)tribenzoate (Me_3btb) adopt a connectivity of eight, with cubic directionality, to yield BUT-12 (Figure 11i), a MOF with the edge-transitive **the** topology.[120] Likewise, the use of other ligands sharing the geometry of Me_3btb, 6,6′,6″-(2,4,6-trimethylbenzene-1,3,5-triyl)tris(2-naphthoate)) (tnna) or 4,4',4''-[benzene-1,3,5-triyl-tris(benzene-4,1-diyl)]tribenzoate (bbc), leads to two other **the**-MOFs: BUT-13[120] and MOF-1005, respectively.[121] Despite the adaptability of the connectivity of the Zr clusters, which helps to form MOFs of highly regular structure and edge-transitive nets, He *et al.* found that use of the highly original T-shaped ligand 4,4′,4″-(1H-benzo[d]imidazole-2,4,7-triyl)tribenzoate (btba) led to a novel, (3,9)-c topology (**sep**) within the Zr/3-c ligand system, as illustrated in their discovery of BUT-39 (Figure 11l).[111]

As we mentioned above, DUT-80 is a unidimensional structure constructed from 8-c Zr clusters and cdc, a ligand with a bend-angle of 90º. Krause *et al.* discovered that using this 1D motif with such an angle implemented in the bcdc ligand leads to an unprecedented (3,12)-c net: they obtained the **llj**-MOF DUT-98 (Figure 11j), which exhibits high structural flexibility.[90]

Another possibility to obtain a novel (3,12)-c net was reported by Lee *et al.* in their construction of MOF-1004, which exhibits the **sky** topology, in which the geometry of the 12-c node is cuboctahedral.[121] To generate this net, they used the wide and slightly flexible ligand 4,4',4''-[benzene-1,3,5-triyltris(ethyne-2,1-diyl)]tribenzoate (bte), in which the angle between two branches is only 94º (compared to 120º in the ideal geometry of the ligand). Interestingly, Sun and co-workers followed this prerequisite in the design of their ligand 4,4',4''-(1H-imidazole-2,4,5-triyl)tribenzoate (ittc), which they subsequently used to assemble UPC-158 (Figure 11k), an isoreticular analog with the **sky** topology.[122]

Their work demonstrates that even such unexpected topologies can be rationally targeted, provided that the geometrical requirements are known.

4.2. Triangular ligands with square paddle wheel building blocks

*In this section, the default topology to assemble regular triangles (equilateral, coplanar carboxylates) with paddle wheels (4-c) is the (3,4)-c edge-transitive **tbo** net. Modifying the coplanarity of the carboxylates, the angles or using ligands with unequal edge-lengths creates geometry mismatch (Figure 12).*

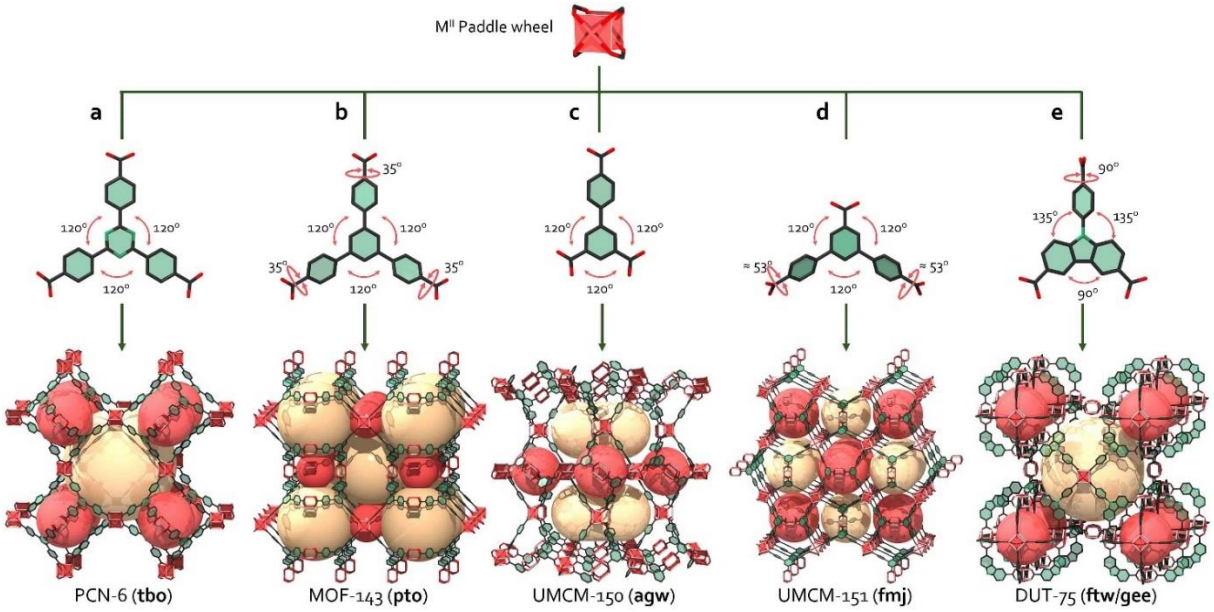

Figure 12. Summary of the Cu-based MOFs resulting from assembly of paddle wheels with triangular ligands. The geometric differences among 3-c ligands strongly influence the resulting MOF structures, leading to the a) **tbo** (PCN-6), b) **pto** (MOF-143), c) **fmj** (UMCM-150), d) **agw** (UMCM-151) or e) **ftw**/**gee** (DUT-75) topologies.

Although the structural and topological variety of MOFs based on paddle wheels and triangular ligands is not as rich as that for hexanuclear clusters and these ligands (*vide supra*), we do consider some examples worthy of discussing here. Combination of a regular planar ligand such as trimesate (btc) with paddle wheels leads to HKUST-1, which exhibits the **tbo** topology;[2] however, obtaining extended reticular analogs is not trivial. Interestingly, using 4,4',4''-benzene-1,3,5-triyl-tris(benzoate) (btb) instead of btc leads to two MOFs that exhibit the **pto** topology, another edge-transitive net: MOF-14[65] (interwoven) and MOF-143[123] (single net, Figure 12b). This is due to the natural twist of the carboxylates in btb. Alternatively, using a fully planar and regular ligand such as 4,4',4"-s-triazine-2,4,6-triyl-tribenzoate (tatb) or 4,4',4''-(benzene-1,3,5-triyl-tris)benzene-4,1-diyltrisbenzoate (bbc), affords the expected **tbo**-MOFs PCN-6 (Figure 12a)[124] or MOF-399,[123] respectively.

Another approach to access unusual topologies from paddle wheels and triangular ligands is simply to elongate one or more ligand branches. For instance, Wong-Foy *et al.* employed biphenyl-3,4,5-tricarboxylate (bptc) to elongate one branch of btc, enabling them to assemble UMCM-150 (Figure 12c), a MOF resulting from the pillaring of Kagomé layers (**kgl**) by a rare Cu trimer to generate the **agw** topology. The layers are constructed from paddle wheels bridged by the isophthalic moieties of the bptc ligands, whereas the remaining benzoic moieties alternately point up or down from the layers, such that another paddle wheel cannot be incorporated, thus "forcing" formation of a 6-c Cu trimer.[125] Lim *et al.* reported that this Cu trimer could be substituted with other metal trimers (Co, Fe, Ni),[126] and Lu *et al.* found that the ligand could be further extended to obtain greater porosity.[127] Similarly, Schnobrich *et al.* used terphenyl tricarboxylate (tptc) to elongate two branches of the btc ligand, ultimately obtaining a UMCM-151 structure that contains paddle wheels only, albeit in an unpredictable, complex, pentanodal (3,3,4,4,4)-c net, **fmj** topology (Figure 12d).[128]

In addition to varying the carboxylate orientation and/or elongating the ligand branches, another approach to obtain dramatically different topologies is to introduce a 90º angle between two branches of the ligand by using carbazole groups, such as those in 4,4′-(9-(4′-carboxy-[1,1′-biphenyl]-4-yl)-9H-carbazole-3,6-diyl)dibenzoate (bpcdc). For example, Stoeck and co-workers rationally designed DUT-75 (Figure 12e) and DUT-76 (**gee** topology) by using the SBB approach to adopt overall **ftw**-type structures.[129] Exploiting the possibility to form carbazole-based MOPs with cuboctahedral shapes,[130] they simply linked the 12-extremities together through a paddle wheel.

4.3. Triangular ligands with 6-c trigonal prismatic building blocks

*In this section, there is no edge-transitive net with which to assemble regular triangles (equilateral, coplanar carboxylates) with 6-c M^{III} (Fe, Al, Cr, Ga, In, etc.) trimers. Given the high incidence of the **moo** net, which derives from the zeolitic **mtn** net, we can consider it to be the default net for these assemblies. Modifying the coplanarity of the carboxylates, the angles using ligands with unequal edge-lengths leads to geometry mismatch (Figure 13).*

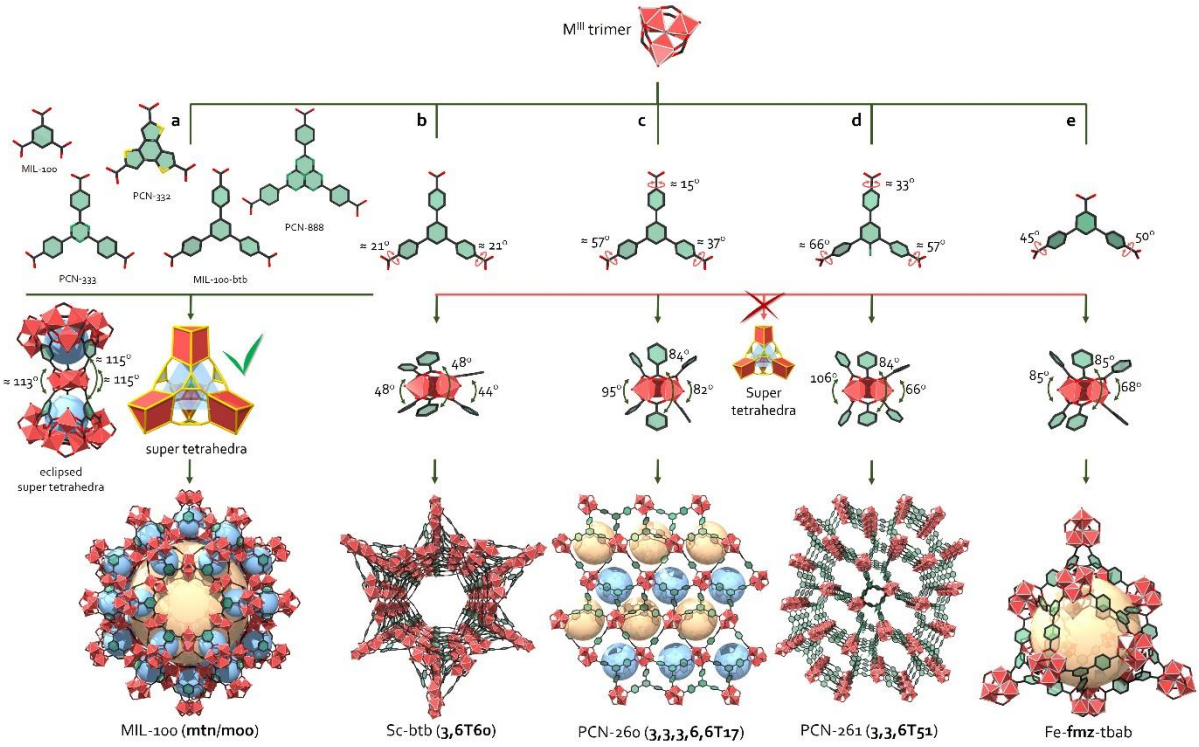

Figure 13. a) Equilateral triangle ligands with coplanar carboxylates assemble with trimers to form supertetrahedra, that further assemble into an underlying zeolitic **mtn** type network (**moo**-MOFs). Breaking the coplanarity leads to other types of MOFs, b) Sc-btb, c) PCN-260 and d) PCN-261), whereas e) using tbab yields the Fe-**fmz**-tbab structure.

Although assembly of regular triangular ligands with 6-c trigonal prismatic MBBs cannot generate an edge-transitive net, various compatible nets with only two types of edges have been reported, including the **ceq**, **dag**, **hwx**, **sit** and **ydq** topologies. Surprisingly, most MOFs in this system adopt the extremely complex, decanodal **moo** topology of MIL-100.[53] This assembly had first been predicted by simulations[131-132] and can be explained by formation of super-tetrahedra that favor further self-assembly of MOFs into an overall zeolitic (**mtn** type) topology, as observed in the examples of MIL-100,[53] MIL-100-btb,[133] PCN-332,[134] PCN-333[134] and PCN-888 (Figure 13a).[135]

Intriguingly, and similarly to other systems that we discuss in this perspective, not all assemblies of regular triangular ligands with 6-c trigonal prisms lead to the **moo** topology. For example, when Ibarra and co-workers assembled btb, which *can* yield **moo** MOFs,[133] with scandium trimers, they instead obtained the MOF Sc-btb (Figure 13b), [136] which exhibits a different topology, (3,6)-c (not described in the RCSR database).[137] This is not surprising, given that the carboxylates from btb are naturally out of

plane, as has been observed in other systems.[33, 65, 119, 138] Additional examples of MOFs constructed from btb (PCN-260, (3,3,3,6,6)-c, not described in the RCSR database,[139] Figure 13c), or amino- (PCN-261, (3,3,6)-c, not described in the RCSR database,[140] Figure 13d) or hydroxyl- (PCN-262) functionalized btb, also derive from the **moo** net. In these MOFs, geometry mismatch again resides in the *natural twist*, for PCN-260 or *forced twist*, for PCN-261 and PCN-262, of the carboxylates.[141]

Although it is difficult to know if it is a parameter governing the topology, or resulting from it, the angles formed by the ligands around the clusters vary significantly from one structure to another, and are far from the *ca.* 115° angle required to form the supertetrahedra necessary for the assembly of **mtn**/**moo** type MOFs (Figure 13).

Another example of geometry mismatch in these systems is to replace btb with a ligand that has one shorter branch (*e.g.* tbab), such that upon assembly of the ligand with the metal trimer, the shorter branch length precludes formation of super-tetrahedra. In this sense, the assembly of tbab with Fe, Ga, In or Al trimers to yield Fe-MOF (Fe-**fmz**-tbab, Figure 13e) and SNNU-5, which exhibit a (3,6)-c net, **fmz** topology.[142-143]

4.4. Triangular ligands with 6-c octahedral building blocks

*In this section, **pyr** is the edge-transitive net to assemble regular triangles with 6-c Zn tetramers ("MOF-5 type" cluster). They require equilateral ligands with highly twisted carboxylate groups of the ligand (i.e. relatively flexible branches). Non-equilateral ligands, ligands with lower coplanarity and ligands with less-twisted carboxylates all generate geometry mismatch (Figure 14).*

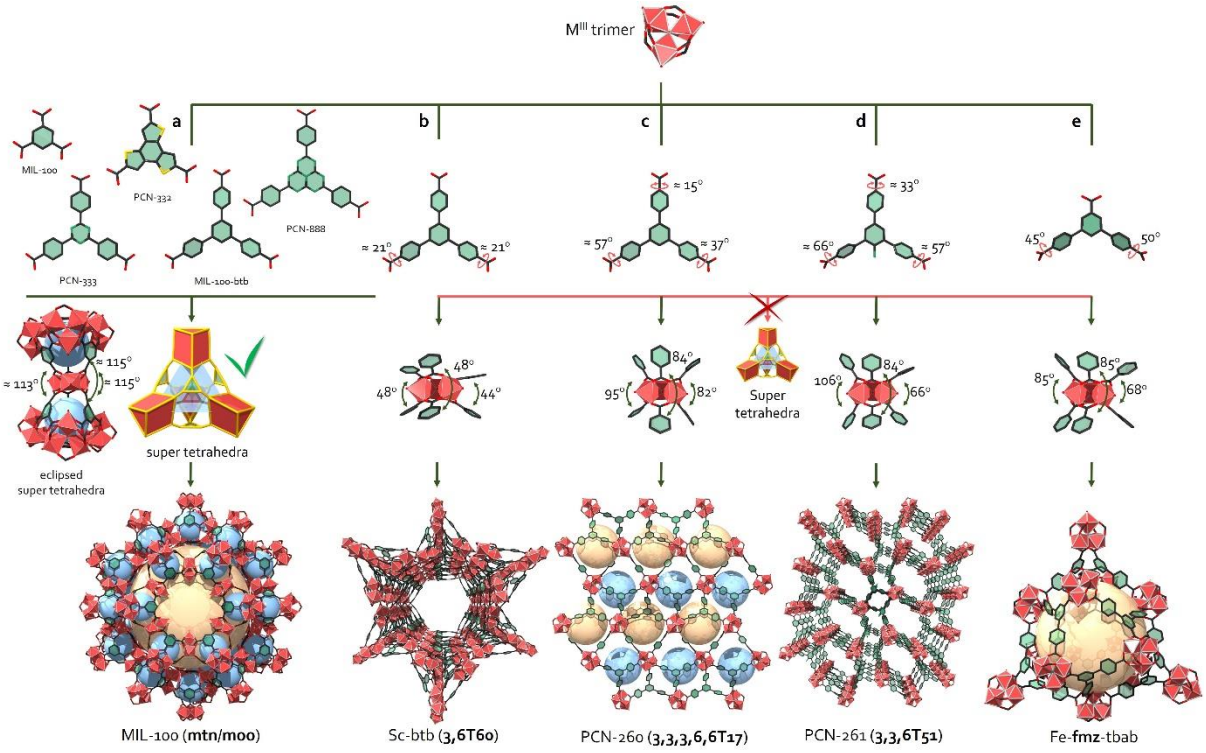

Figure 13. a) Equilateral triangle ligands with coplanar carboxylates assemble with trimers to form supertetrahedra, that further assemble into an underlying zeolitic **mtn** type network (**moo**-MOFs). Breaking the coplanarity leads to other types of MOFs, b) Sc-btb, c) PCN-260 and d) PCN-261), whereas e) using tbab yields the Fe-**fmz**-tbab structure.

There are several examples of regular triangular ligands being assembled with 6-c octahedral Zn tetramers to form **pyr**-MOFs, including MOF-150, constructed with 4,4',4"-tricarboxylate triphenylamine (tca) (Figure 14a);[144] MOF-155-J, built with 1-(3-amino-4-carboxyphenyl)-3-(4-carboxyphenyl)-5-(4-carboxynaphthalen-1-yl)-benzene (btb-*m*NH_2);[145] and MOF-950, made from benzene-1,3,5-tri-β-acryate (btac).[146] However, MOF-177 (Figure 14b),[138] built from btb, and its many (> 20) functionalized[145] or extended analogs,[147] are all based on the "queen of MOFs", the **qom** net. In

these cases, preferential generation of **qom** over **pyr** is due to the weaker twisting of the carboxylates in the ligands used in the **qom** MOFs. However, contrary to a common assumption[138] – and as we explained in the previous paragraph – the carboxylates in the constituent btb ligands of MOF-177 are not coplanar. Another MOF based on different carboxylate twists induced by the use of btb ligand with steric hindrance is MOF-156-J, which exhibits the **rtl** topology (Figure 14c).[145]

In addition to modifying the level of twisting in the ligand carboxylates, other methods to confer systems with geometry mismatch might include altering either the ligand length[148-149] or the angle between the ligand branches[150] (*i.e.* using non-equilateral ligands). The fact that no structure built this way has yet been reported could be explained by the idea that these approaches would likely prevent formation of the Zn tetramer; however, their possible assembly cannot be ruled out.

4.5. Square/rectangle ligands with 4-c paddle wheels building blocks

*In this section, the default topology to assemble square/rectangle ligands with 4-c paddle wheels, is the (3,3,4)-c **fof** net, derived from the edge-transitive **nbo** net (4-c). **fof** MOFs assemble by linking rectangle ligands with two coplanar dicarboxylate groups with a 120° angle (i.e. isophthalate). Breaking this coplanarity or modifying the dicarboxylate angle creates geometry mismatch (Figure 15). Note: this section does not cover examples with ligands based on "naturally tetrahedral" ligands (i.e. containing sp^3 carbon, adamantane central core, etc.).*

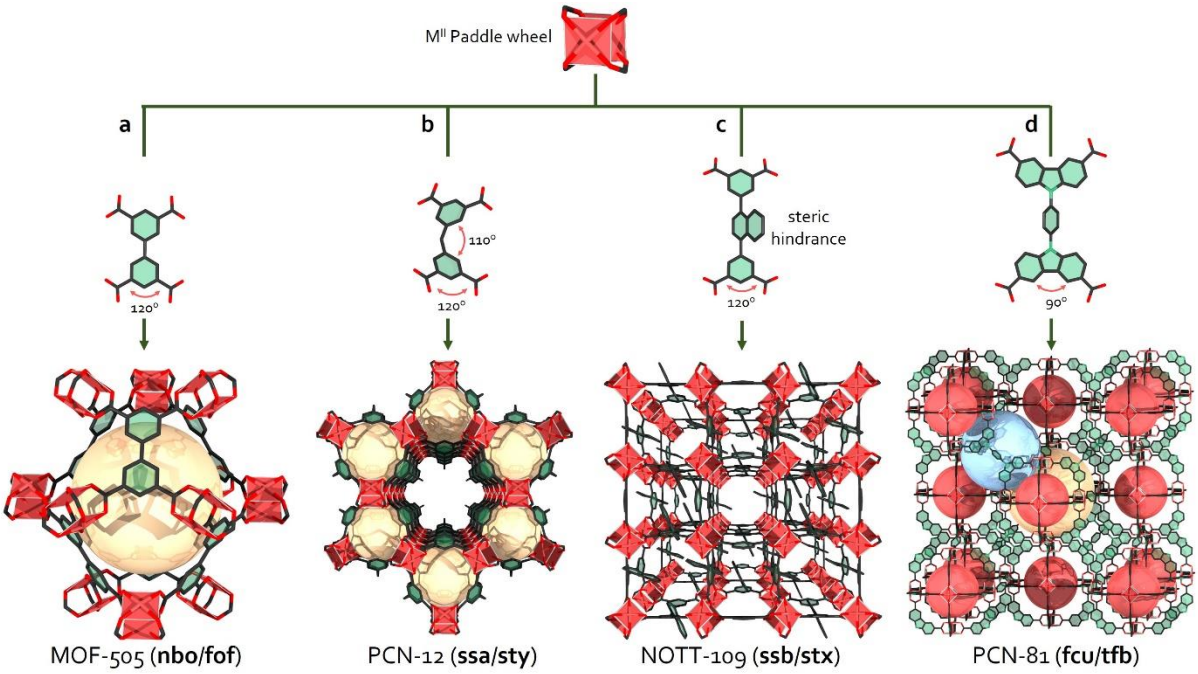

Figure 15. Assembly of paddle wheels with square/rectangular ligands mainly affords a) pillared **kgl** layers in **nbo**/**fof**-type MOFs (MOF-505). b) Introducing bending into the ligand yields a different type of pillaring, leading to the **ssa**/**sty** topology (PCN-12). c) Steric hindrance leads to pillaring **sql** into **ssb**/**stx** MOFs (NOTT-109). d) Reducing the bend-angle from 120º to 90º by replacing isophthalate moieties with carbazoles enables assembly of SBB-based **tfb**-MOF (PCN-81), whose underlying topology is **fcu**.

Numerous MOFs constructed from di-isophthalic-based ligands and paddle wheels have been reported, including MOF-505 (Figure 15a),[151] and their default **nbo**/**fof** topology is widely described in the literature.[4, 152-153] Their structures can be considered as ligand-to-ligand (L-L) pillaring of supermolecular building layers (SBLs).[4] The default SBLs are **kgl**, which are staggered in the **fof** net. Interesting non-default examples include PCN-12 (Figure 15b)[154] and ZJU-25,[155] in which bending of the central core of their respective ligands prevents staggered packing and instead, generates eclipsed pillaring to yield an **ssa**/**sty** topology. Another noteworthy example is NOTT-109 (Figure 15c),[156] in which a bulky naphthalene core precludes formation of the main cage characteristic of **nbo**/**fof** MOFs

and instead, leads to formation of **sql** SBLs, which are pillared in an eclipsed fashion to form the **ssb**/**stx** topology. Researchers have built other pillared **sql** MOFs by using highly flexible ligands.[4, 157] Expectedly, such MOFs may be subject to polymorphism, depending on the ligand conformation.[158-159] Thus, planar (rectangular) ligands lead to an overall **lvt**/**lil** topology, as in DUT-10,[157] whereas tetrahedral analogs of the same ligands (*e.g.* obtained by twisting of the dicarboxylate moieties) lead to the **pts/tfk** topology, as in DUT-11.[157]

Pillaring of SBLs is not the only way to achieve non-default topologies in MOFs assembled from di-isophthalic-based ligands and paddle wheels. As we have discussed above for other MOF families, ligand bend-angles can be chosen to dictate topology. For example, researchers have reported that in SBB assembly with paddle wheels, substituting isophthalate (120º bend) with carbazole dicarboxylate (90º bend) yields PCN-81 (Figure 15d)[160] and DUT-49 with **tfb** topology.[49, 161] In these structures, the dicarboxylate moieties combine with the paddle wheels to form cuboctahedral cages that are bridged by the central core of the ligands to generate the underlying **fcu** topology.

4.6. Square/rectangle ligands with Zr hexanuclear cluster building blocks

*In this section, the default topology to assemble square/rectangle ligands with Zr/Hf/RE hexanuclear clusters ("UiO type cluster") is the edge-transitive (4,12)-c **ftw**. MOFs assemble by linking square ligands with coplanar carboxylate groups. Breaking this coplanarity or deviating from the ideal square shape of the ligand creates geometry mismatch (Figure 16). Note: this section does not cover examples with ligands based on "naturally tetrahedral" ligands (i.e. containing sp^3 carbon, adamantane central core, etc.).*

Beyond the expected **ftw** topology, various other edge-transitive nets have been obtained upon assembly of 4-c ligands with Zr/Hf/RE hexanuclear clusters, including **csq**,[59] **she**,[162] **scu**,[163] **shp**,[164] **flu**,[25] **ith**,[25] **sqc**,[165] **stp**[166] and **lvt**.[167] This is not surprising, given the capacity of such clusters to adapt to lower connectivities (*vide supra*). Many of these topologies resulted when researchers changed the synthetic conditions or the amount of modulator previously used for **ftw** MOFs. Although Chen *et al.* described most of these in their recent review of Zr-MOFs based on edge-transitive nets,[116] we have chosen to highlight a few examples below (Figure 16).

Intriguingly, the **ftw** and **scu** nets are related. The main cage in **ftw**-MOFs can be represented as a cube, in which the clusters lying on the vertices are connected through the 4-c ligands that occupy the faces. Accordingly, elongation of the ligand in a single direction (*i.e.* by using a longer ligand) creates geometry mismatch, as only four of the six faces in the initial cage can accommodate a ligand, leaving the other two free. This scenario favors the **scu**/**tty** topology, in which 1D channels exist and the connectivity of the MBBs is reduced to eight (Figure 16). Moreover, if the length of the longer ligand is moderate compared to its width, as in the case of biphenyl-3,3′,5,5′-tetracarboxylate, bptet,[167] then an **ftw** related MOFs with **kle** topology can still be formed (Figure 16b), as first reported for RE clusters by Luebke *et al.*[168] Along these lines, Wang *et al.*, in their work on replacing the ligand bptet with the longer ligand 3,3′,5,5′-azobenzene-tetracarboxylate (azotet), obtained a rare, **scu**-derived net that is not reported in the RCSR database,[169] in which the ligand orientation alternates and the clusters are tilted from their ideal alignment to balance the ligand length/width ratio (Figure 16c).[167] Interestingly, when they evaluated an even longer ligand, [1,1′:4′,1″]terphenyl- 3,3″,5,5″-tetracarboxylate (tptet), they obtained the first-ever Zr based **lvt/lim**-MOF, in which the connectivity of the Zr cluster is reduced to 4 (Figure 16d).

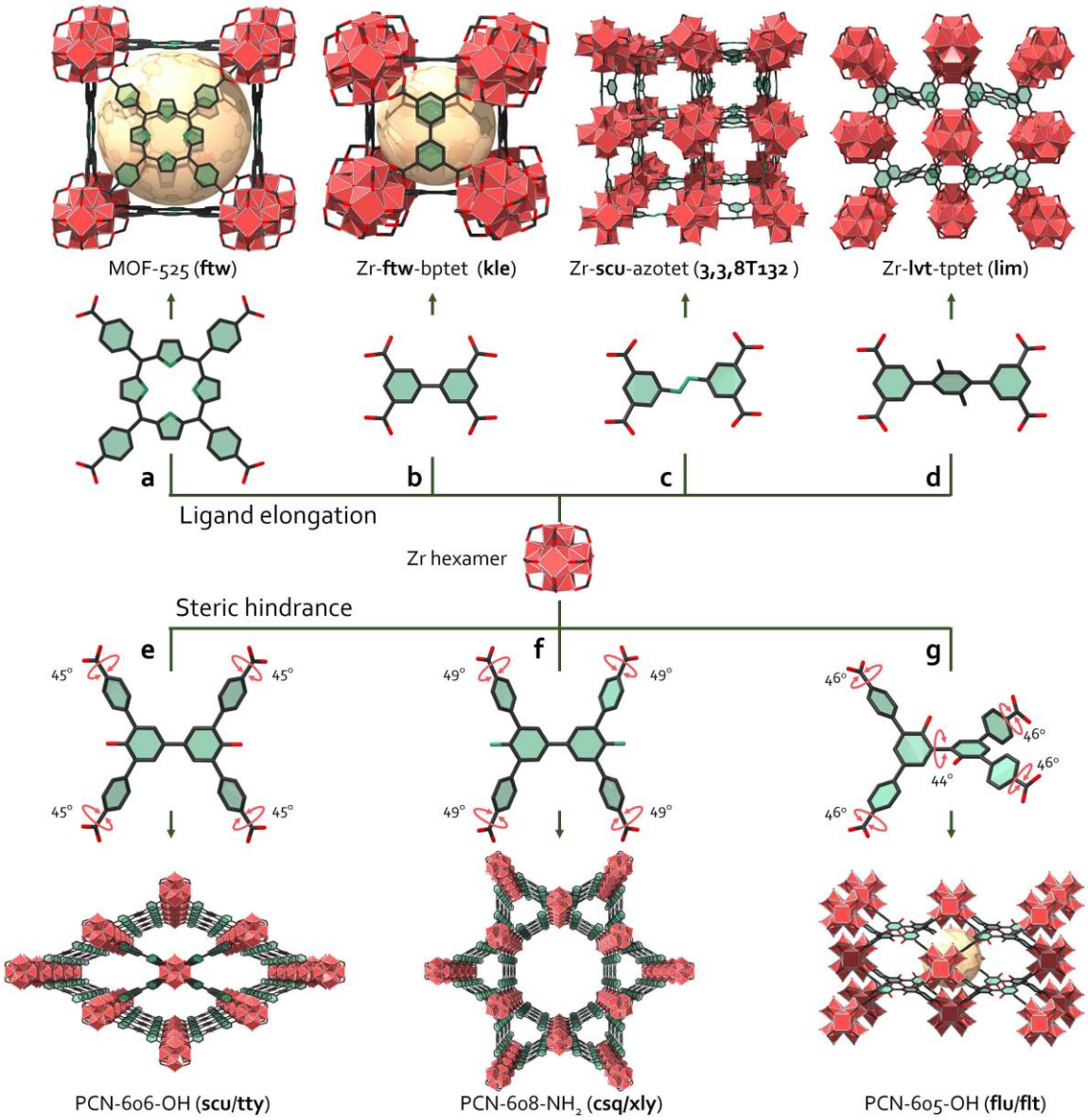

Figure 16. Although assembly of square building blocks with the ideally 12-c connected Zr hexanuclear clusters should lead to the edge-transitive ftw net (MOF-525), elongation of the ligand in one direction can yield **kle**, **scu**/**3,3,8T132** or **lvt**/lim-MOFs. By introducing steric hindrance into a rectangular ligand, the topology can be selectively controlled among **scu**/**tty** (PCN-606), **csq**/**xly** (PCN-608) or, in some cases, **flu**/**flt** (PCN-605).

In most cases, if a ligand's shape deviates significantly from the ideal square shape required for forming an **ftw**-MOF, then the resulting topology will be derived from **csq** (**xly** or **xlz**) or from **scu** (**tty** or **cut**). In some cases, the final geometry of the ligand, and ultimately, the resulting topology, can be controlled by introducing steric hindrance or by using ligands with a less rigid core. Indeed, Pang *et al.* reported selective control among **flu**/**flt** (PCN-605, Figure 16g), **scu**/**tty** (PCN-606, Figure 16e) and **csq**/**xly** (PCN-608, Figure 16f) MOFs, via selective functionalization of a set of 4-c ligands based on 3,3',5,5'-tetra(ethyl-4-carboxyphenyl)-1,1'biphenyl (tpcb).[170] Similarly, Lyu *et al.*, were able to switch from the **scu** net in CAU-24[171] to either the **shp** net in NU-904[172] or the **csq** net in NU-1008,[172] by simply introducing one or two bulky functional groups, respectively, onto the 4,4',4",4"'-benzene-1,2,4,5-tetrayl-tetrabenzoate (tcpb) ligand. These groups directly influence the twisting of the carboxylates and therefore, dictate the resulting topology.

4.7. Hexacarboxylate ligands with 4-c square paddle wheel building blocks: not another rht-MOF

*In this section, the default topology is **ntt**, derived from the edge-transitive (3,24)-c net **rht**. Dicarboxylate bent (120º) extremities of trefoil ligands construct externally functionalized MOPs (24-c), that act as SBBs, and are linked together by the central core of the ligand (3-c). Breaking the planarity of the ligand, or preventing the formation of a 24-c MOP by modifying the angles between carboxylates, each introduces geometry mismatch that precludes formation of **rht**/**ntt**-MOFs (Figure 17).*

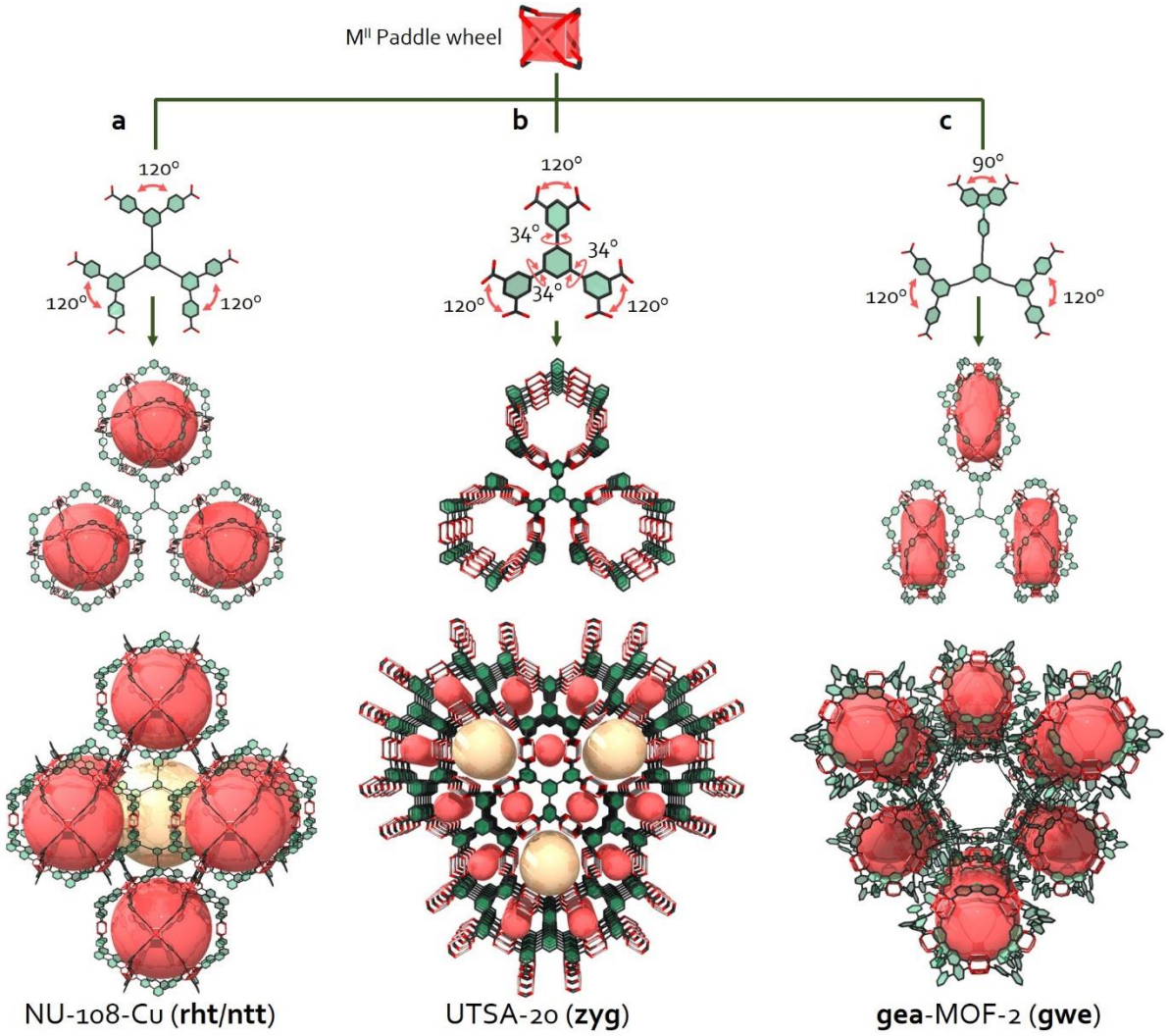

Figure 17. In addition to a) the many **rht**/**ntt**-based MOFs (NU-108-Cu) based on planar hexacarboxylate ligands, one can obtain b) **zyg**-MOF (UTSA-20), by breaking the planarity of the ligand, or c) an SBB-based **gea**/**gwe**-MOF (**gea**-MOF-2), by decreasing (from 120º to 90º) one of the angles in one of the three dicarboxylate moieties, via introduction of carbazole moieties. The latter change leads to an 18-c MOP instead of a 24-c MOP (which would be required to form **rht**/**ntt**-MOFs).

In 2008, Nouar *et al.* described use of externally-functionalized MOPs as SBBs, which they assembled with copper trimers to form **rht**-MOF-1.[40] Interestingly, this trimer can be substituted with 3-connected organic cores[173-174] to afford overall planar hexacarboxylate ligands, which have been used to assemble various **rht**-MOFs (also known as **ntt**-MOFs, Figure 17a) [40, 48, 173, 175-176]. In parallel, Guo *et al.* reported UTSA-20 (Figure 17b), which they built with a similar type of ligand, 3,3',3'',5,5',5''-benzene-1,3,5-triyl-hexabenzoate (bhb), showing that the geometry of this ligand was too intricate and resulted in broken planarity.[177] UTSA-20 exhibits a **zyg** topology and represents one of the rare MOFs based on paddle wheels and hexacarboxylate ligands that does not exhibit the ubiquitous **rht**/**ntt** topology.

Another example of a paddle wheel hexacarboxylate MOF that does not exhibit the **rht** topology is **gea**-MOF-2 (formally: **gwe** topology), a representative case to the scope of this perspective, as the **gea**

topology was discovered by employing a geometry mismatch strategy.[33] Indeed, **gea**-MOF-2 (Figure 17c) was rationally designed using the SBB approach, to specifically adopt an overall **gea** topology. Guillerm *et al.* identified a suitable MOP with 18 vertices[178] matching the geometry of a triangular orthobicupola (**eto**/**ebc**), corresponding to the points of extension of a newly discovered RE nonanuclear cluster with 18 points of extension in **gea**-MOF-1. By incorporating this geometric information to build the **eto**-MOP in a trefoil hexacarboxylic ligand (*i.e.* two 120º angles for one 90º angle), they were able to use the ligand 5′,5□-((5-((4-(3,6-dicarboxylato-9H-carbazol-9-yl)phenyl)ethynyl)-1,3-phenylene)bis(ethyne-2,1-diyl))bis((1,1′:3′,1″-terphenyl]-4,4″-dicarboxylate (lgea2) as a **net**-coded building unit[4] to replicate the underlying **gea** net, enabling its use as a blueprint for rational assembly of **gea**-MOF-2. In this sense, the 90º angle provided geometry mismatch to preclude formation of an **rht**-MOF (for which the 120º angles are crucial).

5. Conclusions

We have provided an overview of geometry mismatch-based approaches to assemble MOFs that exhibit non-default topologies, which in some cases, have enabled discovery of novel clusters that remain to be studied. These approaches obviate classical MOF assembly strategies, in which pre-designed building blocks are used to form specific, edge-transitive or highly regular topologies. Instead, they rely on methods such as transversal reticular chemistry; use of zigzag ligands; introduction of twisting into the ligand carboxylate groups; alteration of ligand bending angles; and changing of the length/width ratio in branched ligands. Thus, by combining classical topology with these strategies to create non-default geometry, researchers are gradually elucidating the pre-requisites for designing MOFs with complex topologies. As researchers have come to understand the basic rules for assembly of some of the topologies previously discovered serendipitously (*e.g.* **gea**, **sky**, **agw**, **pek**, etc.), they have been able to exploit these topologies to further rationally design isoreticular materials.

In several cases, the MBBs are left unsaturated, such that the aforementioned approaches to non-default topologies can be harnessed to construct multivariate MOFs with precisely-positioned functional groups, with the aim of creating functional sequences that mimicking natural structures such as enzymes or DNA.

Finally, given the potential of geometry mismatch to generate countless new MOF topologies and the numerous ways to orient non-linear ligands around a cluster (Figure 6), we consider that human efforts to predict MOF topology are about to reach their limit. Accordingly, we believe that if the MOF research community truly wants to attain the next level of structural complexity in rational design, we must now turn to computational approaches to complement our human efforts. Clearly, such computational tools should be openly available and accessible to theoretical but also experimental scientists in materials science, chemistry and related fields.

ASSOCIATED CONTENT

Supporting information. Summary table of the main structures discussed in this perspective, with topologies, crystallographic information (CCDC codes), corresponding DOI, etc. This material is available free of charge via the Internet at http://pubs.acs.org.

AUTHOR INFORMATION

Corresponding Author

* vincent.guillerm@icn2.cat, daniel.maspoch@icn2.cat

Author Contributions

All authors have given approval to the final version of the manuscript.

ACKNOWLEDGMENT

Prof. Davide M. Proserpio is gratefully acknowledged for fruitful discussion and his help in identifying the net codes of topologies not registered in the RCSR database.

Dr. Volodymyr Bon and Dr. Feng Liang are acknowledged for their help regarding the signification of some topology acronyms.
Borja Ortín-Rubio is acknowledged for his helpful comments on a preliminary version of the perspective.
The authors acknowledge the reviewers for their critical and constructive comments, they helped to improve this perspective.

NOTES

In this perspective, we consider the default net to be the one with edge transitivity or minimal transitivity, and the node corresponding to the inorganic cluster matching its ideal connectivity. In case several edge-transitive exist for assembling similar building blocks (**sql** *vs* **nbo**; **tbo** *vs* **pto**, etc.), the net chosen as default is the one for which the ligands have higher symmetry in the corresponding structures.
In various cases, the topology used to design specific MOFs, or the reported topology, do not match those obtained by following the recommendations of O'Keeffe and coworkers, on using derived nets. For such cases, we have denoted both topologies in the text (e.g. **rht**/**ntt**, **ftw**/**gee**, **fcu**/**tfb**, **nbo**/**fof**, etc.). Figure S1 represents several examples of such MOFs described in two different ways.
There are several occurrences of MOFs discussed in this perspective that do not have their topology registered in the RCSR database. They have been identified using ToposPro[30] and we refer to them using the TopCryst codes (https://topcryst.com/).
In the case several crystallographically independent ligands are present in a structure, ranges of bend angle or average twist/torsion angle are reported in this perspective.

ABBREVIATIONS

General acronyms (order of appearance): MOF, metal-organic framework; MBB, molecular building block; SBU, secondary building unit; IRMOF, isoreticular MOF; RCSR, reticular chemistry structure resource; SBB, supermolecular building block; RE, rare earth; MOP, metal-organic polyhedra; L-L, ligand-to-ligand; SBL, supermolecular building layer; DNA, deoxyribonucleic acid.

Materials acronyms (order of appearance): HKUST, Hong Kong University of Science and Technology; MOF, Metal-Organic Framework; MIL, Material Institute Lavoisier; UiO, Universitetet i Oslo; DUT, Dresden University of Technology; JLU, Jilin University; CAU, Christian Albrechts University; BUT, Beijing University of Technology; MIP, Materials from Institute of porous materials of Paris; PCN, porous coordination network; UPC, University of Petroleum, Qingdao, China; UMCM, University of Michigan crystalline material; SNNU, Shangqiu Normal University; ZJU, Zhejiang University; NOTT, Nottingham; NU, Northwestern University; UTSA, the University of Texas at San Antonio.

Ligands acronyms (order of appearance): tcpp, tetrakis(4-carboxyphenyl)porphyrin; bdc, terephthalate; Br-bdc, bromo-terephthalate; Me_2bpdc, 2,2′-dimethyl biphenyl-4,4′-dicarboxylate; pdi, N,N′-di-(4-benzate)-1,2,6,7-tetrachloroperylene-3,4,9,10-tetracarboxylic acid diimide; fldc, 9□fluoreneone□2,7□ dicarboxylate; dttdc, dithienothiophene dicarboxylate; tadiba, 4,4'-(2 H-1,2,4-triazole-3,5-diyl) dibenzoate; tdc, 2,5-thiophenedicarboxylate; pzdc, 3,5-pyrazoledicarboxylate; fdc, 2,5-furandicarboxylic; *m*-bdc, isophthalate; bdb, 4,4'-(benzene-1,3-diyl)dibenzoate; ndb, 4,4'-(naphthalene-2,7-diyl)dibenzoate; *m*-bdc-F_4, tetrafluoroisophthalate; cdc, 9h-Carbazole-3,6-dicarboxylate; tmuc, *trans, trans* muconate; 26ndc, 2,6-naphthalene dicarboxylate; 22bipy44dc, 2 2'-bipyridine-4 4'-dicarboxylate; azo33, azobenzene-3 3'-dicarboxylate; suc, succinate; azo44, azobenzene-4 4'-dicarboxylate; 44bpdc, 4,4'-biphenyldicarboxylate; btb, 4,4′,4″,-benzene-1,3,5-triyl-trisbenzoate; bcdc, 9-(4-carboxyphenyl)-9H-carbazole-3,6-dicarboxylate; bptc, [1,1'-biphenyl]-3,4',5-tricarboxylate; obi, 5-(4-carboxybenzyloxy)isophthalate; tptc, [1,1':3',1"-terphenyl]-4,4",5'-tricarboxylate; btc, trimesate; tatb, 4,4′,4″-s-Triazine-2,4,6-triyl-tribenzoate; Me_3btb, 4,4',4''-(2,4,6-trimethyl-benzene-1,3,5-triyl)tribenzoate; tnna, 6,6′,6″-(2,4,6-trimethylbenzene-1,3,5-triyl)tris(2-naphthoate)); bbc, 4,4',4''-[benzene-1,3,5-triyl-tris(benzene-4,1-diyl)]tribenzoate; btba, 4,4′,4″-(1H-benzo[d]imidazole-2,4,7-triyl)tribenzoate; bte, 4,4',4''-[benzene-1,3,5-triyltris(ethyne-2,1-diyl)]tribenzoate; ittc, 4,4',4''-(1H-imidazole-2,4,5-triyl)tribenzoate; bpcdc, 4,4′-(9-(4′-carboxy-[1,1′-biphenyl]-4-yl)-9*H*-carbazole-3,6-

diyl)dibenzoate; tca, 4,4',4"- tricarboxylate triphenylamine; btb-*m*NH_2, 1-(3-amino-4-carboxyphenyl)-3-(4-carboxyphenyl)-5-(4-carboxynaphthalen-1-yl)-benzene; btac, benzene-1,3,5-tri-β-acryate; bptet, biphenyl-3,3′,5,5′-tetracarboxylate; azotet, 3,3′,5,5′-azobenzene-tetracarboxylate; tptet, [1,1′:4′,1″]terphenyl- 3,3″,5,5″-tetracarboxylate; tpcb, 3,3’,5,5’-tetra(ethyl-4-carboxyphenyl)-1,1’biphenyl; tcpb, 4,4',4",4"'-benzene-1,2,4,5-tetrayl-tetrabenzoate; bhb, ,3’,3”,5,5’,5”-benzene-1,3,5-triyl-hexabenzoate; lnu108, 1,3,5-tris[(1,3-di(4'-carboxylate-phenyl)-phenyl)-5-ethynyl]benzene; lgea2, 5′,5□-((5-((4-(3,6-dicarboxylato-9H-carbazol-9-yl)phenyl)ethynyl)-1,3-phenylene)bis(ethyne-2,1-diyl))bis((1,1′:3′,1″-terphenyl]-4,4″-dicarboxylate)

Topology acronyms (order of appearance): **rht**, rhombicuboctahedron, triangle; **ith**, icosahedron, tetrahedron; **ftw**, four, twelve; **shp**, square, hexagonal prism; **fcu**, face centered cubic; **sql**, square lattice; **nbo**, Nb_2O_5; **cds**, $CdSO_4$; **bcu**, body centered cubic; **dia**, diamond; **kgm**, Kagomé lattice; **reo**, ReO_3; **bon**, Volodymyr Bon; **bct**, body centered tetragonal; **kag**, Kagomé net; **pcu**, primitive cubic; **gea**, Guillerm, Eddaoudi, net A; **aea**, Alezi, Eddaoudi, net A; **pek**, Puthan Peedikakkal, Eddaoudi, Kaust; **flg**, Feng Liang; **ytw**, Yutong Wang; **sep**, september; **csq**, cube, square; **spn**, spinel; **kgd**, Kagomé dual; **the**, three, eight; **tbo**, twisted boracite; **agw**, Antek G. Wong-Foy; **gee**, Guillerm, Eddaoudi, net E; **moo**, MIL-100; **mtn**, MTN zeolite type; **fmz**, Feng Ming Zhang; **pyr**, pyrite; **qom**, Queen of MOFs; **rtl**, rutile; , **ssa**, square, square, net A, **sty**, square, triangles axis Y; **ssb**, square, square, net B; **stx**, , square, triangles axis X; **lvt**, lattice complex ^{v}T; **pts**, PtS; **she**, square, hexagon; **scu**, square, cube; **flu**, fluorite; **sqc**, square, cube; **stp**, square, trigonal prism; **kle**, Kaust, Luebke, Eddaoudi; **cut**, cube, triangle; **flt**, fluorite, triangle **ntt**, Nottingham; **zyg**, Zhiyong Guo; **gwe**, Guillerm, Weseliński, Eddaoudi.
We could not identify the correspondence for the following topology acronyms: **hbr**, **nht**, **llj**, **sky**, **fmj**, **ceq**, **dag**, **hwx**, **sit**, **ydq**, **fof**, **lil**, **tfk**, **tfb**, **lim**, **tty**, **xly**, **xlz**.

REFERENCES

1. Li, H.; Eddaoudi, M.; O'Keeffe, M.; Yaghi, O. M., Design and synthesis of an exceptionally stable and highly porous metal-organic framework. *Nature* **1999,** *402* (6759), 276-279.

2. Chui, S. S. Y.; Lo, S. M. F.; Charmant, J. P. H.; Orpen, A. G.; Williams, I. D., A chemically functionalizable nanoporous material $[Cu_3(TMA)_2(H_2O)_3]_n$. *Science* **1999,** *283* (5405), 1148-1150.

3. Furukawa, H.; Cordova, K. E.; O’Keeffe, M.; Yaghi, O. M., The Chemistry and Applications of Metal-Organic Frameworks. *Science* **2013,** *341* (6149).

4. Guillerm, V.; Kim, D.; Eubank, J. F.; Luebke, R.; Liu, X.; Adil, K.; Lah, M. S.; Eddaoudi, M., A supermolecular building approach for the design and construction of metal-organic frameworks. *Chem. Soc. Rev.* **2014,** *43* (16), 6141-6172.

5. Subramanian, S.; Zaworotko, M. J., Porous Solids by Design: $[Zn(4,4'\text{-bpy})_2(SiF_6)]_n \cdot xDMF$, a Single Framework Octahedral Coordination Polymer with Large Square Channels. *Angew. Chem., Int. Ed.* **1995,** *34* (19), 2127-2129.

6. O'Keeffe, M.; Eddaoudi, M.; Li, H. L.; Reineke, T. M.; Yaghi, O. M., Frameworks for extended solids: Geometrical design principles. *J. Solid State Chem.* **2000,** *152* (1), 3-20.

7. Eddaoudi, M.; Moler, D. B.; Li, H. L.; Chen, B. L.; Reineke, T. M.; O'Keeffe, M.; Yaghi, O. M., Modular chemistry: Secondary building units as a basis for the design of highly porous and robust metal-organic carboxylate frameworks. *Acc. Chem. Res.* **2001,** *34* (4), 319-330.

8. Yaghi, O. M.; O'Keeffe, M.; Ockwig, N. W.; Chae, H. K.; Eddaoudi, M.; Kim, J., Reticular synthesis and the design of new materials. *Nature* **2003,** *423* (6941), 705-714.

9. Jiang, H.; Jia, J.; Shkurenko, A.; Chen, Z.; Adil, K.; Belmabkhout, Y.; Weselinski, L. J.; Assen, A. H.; Xue, D.-X.; O'Keeffe, M.; Eddaoudi, M., Enriching the Reticular Chemistry Repertoire: Merged Nets Approach for the Rational Design of Intricate Mixed-Linker Metal–Organic Framework Platforms. *J. Am. Chem. Soc.* **2018,** *140* (28), 8858-8867.

10. Tranchemontagne, D. J.; Mendoza-Cortes, J. L.; O'Keeffe, M.; Yaghi, O. M., Secondary building units, nets and bonding in the chemistry of metal-organic frameworks. *Chem. Soc. Rev.* **2009,** *38* (5), 1257-1283.

11. Delgado-Friedrichs, O.; O'Keeffe, M.; Yaghi, O. M., Three-periodic nets and tilings: edge-transitive binodal structures. *Acta Cryst. A* **2006,** *62*, 350-355.

12. Delgado-Friedrichs, O.; O'Keeffe, M., Three-periodic tilings and nets: face-transitive tilings and edge-transitive nets revisited. *Acta Cryst. A* **2007,** *63* (4), 344-347.

13. Li, M.; Li, D.; O'Keeffe, M.; Yaghi, O. M., Topological Analysis of Metal–Organic Frameworks with Polytopic Linkers and/or Multiple Building Units and the Minimal Transitivity Principle. *Chem. Rev.* **2014,** *114* (2), 1343-1370.

14. O'Keeffe, M.; Yaghi, O. M., Deconstructing the Crystal Structures of Metal-Organic Frameworks and Related Materials into Their Underlying Nets. *Chem. Rev.* **2012,** *112* (2), 675-702.

15. Belmabkhout, Y.; Guillerm, V.; Eddaoudi, M., Low concentration CO_2 capture using physical adsorbents: Are metal–organic frameworks becoming the new benchmark materials? *Chem. Eng. J.* **2016,** *296*, 386-397.

16. Belmabkhout, Y.; Mouttaki, H.; Eubank, J. F.; Guillerm, V.; Eddaoudi, M., Effect of pendant isophthalic acid moieties on the adsorption properties of light hydrocarbons in HKUST-1-like tbo-MOFs: Application to methane purification and storage. *RSC Adv.* **2014,** *4* (109), 63855-63859.

17. Shekhah, O.; Belmabkhout, Y.; Chen, Z.; Guillerm, V.; Cairns, A.; Adil, K.; Eddaoudi, M., Made-to-order metal-organic frameworks for trace carbon dioxide removal and air capture. *Nat. Commun.* **2014,** *5* (1), 4228.

18. Li, H.; Wang, K.; Sun, Y.; Lollar, C. T.; Li, J.; Zhou, H.-C., Recent advances in gas storage and separation using metal–organic frameworks. *Mater. Today* **2018,** *21* (2), 108-121.

19. Li, J.; Wang, X.; Zhao, G.; Chen, C.; Chai, Z.; Alsaedi, A.; Hayat, T.; Wang, X., Metal–organic framework-based materials: superior adsorbents for the capture of toxic and radioactive metal ions. *Chem. Soc. Rev.* **2018,** *47* (7), 2322-2356.

20. Sun, D. T.; Gasilova, N.; Yang, S.; Oveisi, E.; Queen, W. L., Rapid, Selective Extraction of Trace Amounts of Gold from Complex Water Mixtures with a Metal–Organic Framework (MOF)/Polymer Composite. *J. Am. Chem. Soc.* **2018,** *140* (48), 16697-16703.

21. Kim, H.; Rao, S. R.; Kapustin, E. A.; Zhao, L.; Yang, S.; Yaghi, O. M.; Wang, E. N., Adsorption-based atmospheric water harvesting device for arid climates. *Nat. Commun.* **2018,** *9* (1), 1191.

22. Kim, H.; Yang, S.; Rao, S. R.; Narayanan, S.; Kapustin, E. A.; Furukawa, H.; Umans, A. S.; Yaghi, O. M.; Wang, E. N., Water harvesting from air with metal-organic frameworks powered by natural sunlight. *Science* **2017,** *356* (6336), 430-434.

23. Kalmutzki, M. J.; Diercks, C. S.; Yaghi, O. M., Metal–Organic Frameworks for Water Harvesting from Air. *Adv. Mater.* **2018,** *30* (37), 1704304.

24. Garzón-Tovar, L.; Pérez-Carvajal, J.; Imaz, I.; Maspoch, D., Composite Salt in Porous Metal-Organic Frameworks for Adsorption Heat Transformation. *Adv. Funct. Mater.* **2017,** *27* (21), 1606424.

25. Furukawa, H.; Gándara, F.; Zhang, Y.-B.; Jiang, J.; Queen, W. L.; Hudson, M. R.; Yaghi, O. M., Water Adsorption in Porous Metal–Organic Frameworks and Related Materials. *J. Am. Chem. Soc.* **2014,** *136* (11), 4369-4381.

26. Troyano, J.; Carné-Sánchez, A.; Pérez-Carvajal, J.; León-Reina, L.; Imaz, I.; Cabeza, A.; Maspoch, D., A Self-Folding Polymer Film Based on Swelling Metal–Organic Frameworks. *Angew. Chem., Int. Ed.* **2018,** *57* (47), 15420-15424.

27. Wang, X.; Chen, X.-Z.; Alcântara, C. C. J.; Sevim, S.; Hoop, M.; Terzopoulou, A.; de Marco, C.; Hu, C.; de Mello, A. J.; Falcaro, P.; Furukawa, S.; Nelson, B. J.; Puigmartí-Luis, J.; Pané, S., MOFBOTS: Metal–Organic-Framework-Based Biomedical Microrobots. *Adv. Mater.* **2019**, 1901592.

28. Troyano, J.; Carné-Sánchez, A.; Maspoch, D., Programmable Self-Assembling 3D Architectures Generated by Patterning of Swellable MOF-Based Composite Films. *Adv. Mater.* **2019,** *31* (21), 1808235.

29. O'Keeffe, M.; Peskov, M. A.; Ramsden, S. J.; Yaghi, O. M., The Reticular Chemistry Structure Resource (RCSR) Database of, and Symbols for, Crystal Nets. *Acc. Chem. Res.* **2008,** *41* (12), 1782-1789.

30. Blatov, V. A.; Shevchenko, A. P.; Proserpio, D. M., Applied Topological Analysis of Crystal Structures with the Program Package ToposPro. *Cryst. Growth Des.* **2014,** *14* (7), 3576-3586.

31. Moghadam, P. Z.; Li, A.; Wiggin, S. B.; Tao, A.; Maloney, A. G. P.; Wood, P. A.; Ward, S. C.; Fairen-Jimenez, D., Development of a Cambridge Structural Database Subset: A Collection of Metal–Organic Frameworks for Past, Present, and Future. *Chem. Mater.* **2017,** *29* (7), 2618-2625.

32. Eddaoudi, M., *Unpublished results*.

33. Guillerm, V.; Weseliński, Ł. J.; Belmabkhout, Y.; Cairns, A. J.; D'Elia, V.; Wojtas, Ł.; Adil, K.; Eddaoudi, M., Discovery and introduction of a (3,18)-connected net as an ideal blueprint for the design of metal-organic frameworks. *Nat. Chem.* **2014,** *6* (8), 673-680.

34. Yuan, S.; Qin, J.-S.; Lollar, C. T.; Zhou, H.-C., Stable Metal–Organic Frameworks with Group 4 Metals: Current Status and Trends. *ACS Cent. Sci.* **2018,** *4* (4), 440-450.

35. Alezi, D.; Peedikakkal, A. M. P.; Weseliński, Ł. J.; Guillerm, V.; Belmabkhout, Y.; Cairns, A. J.; Chen, Z.; Wojtas, Ł.; Eddaoudi, M., Quest for Highly Connected Metal–Organic Framework Platforms: Rare-Earth Polynuclear Clusters Versatility Meets Net Topology Needs. *J. Am. Chem. Soc.* **2015,** *137* (16), 5421-5430.

36. Feng, D.; Jiang, H.-L.; Chen, Y.-P.; Gu, Z.-Y.; Wei, Z.; Zhou, H.-C., Metal–Organic Frameworks Based on Previously Unknown Zr_8/Hf_8 Cubic Clusters. *Inorg. Chem.* **2013,** *52* (21), 12661-12667.

37. Furukawa, H.; Kim, J.; Ockwig, N. W.; O'Keeffe, M.; Yaghi, O. M., Control of vertex geometry, structure dimensionality, functionality, and pore metrics in the reticular synthesis of crystalline metal-organic frameworks and polyhedra. *J. Am. Chem. Soc.* **2008,** *130* (35), 11650-11661.

38. Eddaoudi, M.; Kim, J.; Vodak, D.; Sudik, A.; Wachter, J.; O'Keeffe, M.; Yaghi, O. M., Geometric requirements and examples of important structures in the assembly of square building blocks. *Proc. Nat. Acad. Sci. USA* **2002,** *99* (8), 4900-4904.

39. http://europe.iza-structure.org/IZA-SC/ftc_table.php (accessed 29-jul-19).

40. Nouar, F.; Eubank, J. F.; Bousquet, T.; Wojtas, Ł.; Zaworotko, M. J.; Eddaoudi, M., Supermolecular building blocks (SBBs) for the design and synthesis of highly porous metal-organic frameworks. *J. Am. Chem. Soc.* **2008,** *130* (6), 1833-1834.

41. Guillerm, V.; Gross, S.; Serre, C.; Devic, T.; Bauer, M.; Férey, G., A zirconium methacrylate oxocluster as precursor for the low-temperature synthesis of porous zirconium(IV) dicarboxylates. *Chem. Commun.* **2010,** *46* (5), 767-769.

42. Dan-Hardi, M.; Serre, C.; Frot, T.; Rozes, L.; Maurin, G.; Sanchez, C.; Férey, G., A New Photoactive Crystalline Highly Porous Titanium(IV) Dicarboxylate. *J. Am. Chem. Soc.* **2009,** *131* (31), 10857-10859.

43. Xue, D.-X.; Cairns, A. J.; Belmabkhout, Y.; Wojtas, Ł.; Liu, Y.; Alkordi, M. H.; Eddaoudi, M., Tunable Rare-Earth fcu-MOFs: A Platform for Systematic Enhancement of CO2 Adsorption Energetics and Uptake. *J. Am. Chem. Soc.* **2013,** *135* (20), 7660-7.

44. Wang, Y.; Feng, L.; Fan, W.; Wang, K.-Y.; Wang, X.; Wang, X.; Zhang, K.; Zhang, X.; Dai, F.; Sun, D.; Zhou, H.-C., Topology Exploration in Highly Connected Rare-Earth Metal–Organic Frameworks via Continuous Hindrance Control. *J. Am. Chem. Soc.* **2019,** *141* (17), 6967-6975.

45. Ahnfeldt, T.; Guillou, N.; Gunzelmann, D.; Margiolaki, I.; Loiseau, T.; Férey, G.; Senker, J.; Stock, N., $[Al_4(OH)_2(OCH_3)_4(H_2N\text{-}bdc)_3]\cdot x\ H_2O$: A 12-Connected Porous Metal–Organic Framework with an Unprecedented Aluminum-Containing Brick. *Angew. Chem., Int. Ed.* **2009,** *48* (28), 5163-5166.

46. Padial, N. M.; Quartapelle Procopio, E.; Montoro, C.; López, E.; Oltra, J. E.; Colombo, V.; Maspero, A.; Masciocchi, N.; Galli, S.; Senkovska, I.; Kaskel, S.; Barea, E.; Navarro, J. A. R., Highly Hydrophobic Isoreticular Porous Metal–Organic Frameworks for the Capture of Harmful Volatile Organic Compounds. *Angew. Chem., Int. Ed.* **2013,** *52* (32), 8290-8294.

47. Du, D.-Y.; Qin, J.-S.; Sun, Z.; Yan, L.-K.; O'Keeffe, M.; Su, Z.-M.; Li, S.-L.; Wang, X.-H.; Wang, X.-L.; Lan, Y.-Q., An unprecedented (3,4,24)-connected heteropolyoxozincate organic framework as heterogeneous crystalline Lewis acid catalyst for biodiesel production. *Sci. Rep.* **2013,** *3*, 2616.

48. Eubank, J. F.; Nouar, F.; Luebke, R.; Cairns, A. J.; Wojtas, Ł.; Alkordi, M.; Bousquet, T.; Hight, M. R.; Eckert, J.; Embs, J. P.; Georgiev, P. A.; Eddaoudi, M., On Demand: The Singular rht Net, an Ideal Blueprint for the Construction of a Metal–Organic Framework (MOF) Platform. *Angew. Chem., Int. Ed.* **2012,** *51* (40), 10099-10103.

49. Stoeck, U.; Krause, S.; Bon, V.; Senkovska, I.; Kaskel, S., A highly porous metal-organic framework, constructed from a cuboctahedral super-molecular building block, with exceptionally high methane uptake. *Chem. Commun.* **2012,** *48* (88), 10841-10843.

50. Eddaoudi, M.; Kim, J.; O'Keeffe, M.; Yaghi, O. M., $Cu_2[o\text{-}Br\text{-}C_6H_3(CO_2)_2]_2(H_2O)_2\cdot(DMF)_8(H_2O)_2$: A Framework Deliberately Designed To Have the NbO Structure Type. *J. Am. Chem. Soc.* **2002,** *124* (3), 376-377.

51. Guillerm, V.; Grancha, T.; Imaz, I.; Juanhuix, J.; Maspoch, D., Zigzag Ligands for Transversal Design in Reticular Chemistry: Unveiling New Structural Opportunities for Metal–Organic Frameworks. *J. Am. Chem. Soc.* **2018,** *140* (32), 10153-10157.

52. Groom, C. R.; Bruno, I. J.; Lightfoot, M. P.; Ward, S. C., The Cambridge Structural Database. *Acta Cryst. B* **2016,** *72* (2), 171-179.

53. Férey, G.; Serre, C.; Mellot-Draznieks, C.; Millange, F.; Surblé, S.; Dutour, J.; Margiolaki, I., A hybrid solid with giant pores prepared by a combination of targeted chemistry, simulation, and powder diffraction. *Angew. Chem., Int. Ed.* **2004,** *43* (46), 6296-6301.

54. Cavka, J. H.; Jakobsen, S.; Olsbye, U.; Guillou, N.; Lamberti, C.; Bordiga, S.; Lillerud, K. P., A new zirconium inorganic building brick forming metal organic frameworks with exceptional stability. *J. Am. Chem. Soc.* **2008,** *130* (42), 13850-13851.

55. Delgado Friedrichs, O.; O'Keeffe, M.; Yaghi, O. M., Three-periodic nets and tilings: semiregular nets. *Acta Cryst. A* **2003,** *59* (6), 515-525.

56. Delgado Friedrichs, O.; O'Keeffe, M.; Yaghi, O. M., Three-periodic nets and tilings: regular and quasiregular nets. *Acta Cryst. A* **2003,** *59* (1), 22-27.

57. Delgado-Friedrichs, O.; Foster, M. D.; O'Keeffe, M.; Proserpio, D. M.; Treacy, M. M. J.; Yaghi, O. M., What do we know about three-periodic nets? *J. Solid State Chem.* **2005,** *178* (8), 2533-2554.

58. Delgado-Friedrichs, O.; O'Keeffe, M.; Yaghi, O. M., Taxonomy of periodic nets and the design of materials. *Phys. Chem. Chem. Phys.* **2007,** *9* (9), 1035-1043.

59. Morris, W.; Volosskiy, B.; Demir, S.; Gándara, F.; McGrier, P. L.; Furukawa, H.; Cascio, D.; Stoddart, J. F.; Yaghi, O. M., Synthesis, Structure, and Metalation of Two New Highly Porous Zirconium Metal-Organic Frameworks. *Inorg. Chem.* **2012,** *51* (12), 6443-6445.

60. Eddaoudi, M.; Kim, J.; Rosi, N.; Vodak, D.; Wachter, J.; O'Keeffe, M.; Yaghi, O. M., Systematic design of pore size and functionality in isoreticular MOFs and their application in methane storage. *Science* **2002,** *295* (5554), 469-472.

61. Abrahams, B. F.; Batten, S. R.; Hamit, H.; Hoskins, B. F.; Robson, R., A Cubic (3,4)-Connected Net with Large Cavities in Solvated $[Cu_3(tpt)_4](ClO_4)_3$ (tpt = 2,4,6-Tri(4-pyridyl)-1,3,5-triazine). *Angew. Chem., Int. Ed.* **1996,** *35* (15), 1690-1692.

62. Mori, W.; Inoue, F.; Yoshida, K.; Nakayama, H.; Takamizawa, S.; Kishita, M., Synthesis of New Adsorbent Copper(II) Terephthalate. *Chem. Letters* **1997,** *26* (12), 1219-1220.

63. Yaghi, O. M.; Davis, C. E.; Li, G.; Li, H., Selective Guest Binding by Tailored Channels in a 3-D Porous Zinc(II)−Benzenetricarboxylate Network. *J. Am. Chem. Soc.* **1997,** *119* (12), 2861-2868.

64. Li, H.; Eddaoudi, M.; Groy, T. L.; Yaghi, O. M., Establishing microporosity in open metal-organic frameworks: Gas sorption isotherms for Zn(BDC) (BDC = 1,4-benzenedicarboxylate). *J. Am. Chem. Soc.* **1998,** *120* (33), 8571-8572.

65. Chen, B.; Eddaoudi, M.; Hyde, S. T.; O'Keeffe, M.; Yaghi, O. M., Interwoven Metal-Organic Framework on a Periodic Minimal Surface with Extra-Large Pores. *Science* **2001,** *291* (5506), 1021-1023.

66. Yuan, S.; Chen, Y.-P.; Qin, J.-S.; Lu, W.; Zou, L.; Zhang, Q.; Wang, X.; Sun, X.; Zhou, H.-C., Linker Installation: Engineering Pore Environment with Precisely Placed Functionalities in Zirconium MOFs. *J. Am. Chem. Soc.* **2016,** *138* (28), 8912-8919.

67. Yuan, S.; Zou, L.; Li, H.; Chen, Y. P.; Qin, J.; Zhang, Q.; Lu, W.; Hall, M. B.; Zhou, H. C., Flexible Zirconium Metal□Organic Frameworks as Bioinspired Switchable Catalysts. *Angew. Chem., Int. Ed.* **2016,** *55* (36), 10776-10780.

68. Chen, C. X.; Wei, Z.; Jiang, J. J.; Fan, Y. Z.; Zheng, S. P.; Cao, C. C.; Li, Y. H.; Fenske, D.; Su, C. Y., Precise Modulation of the Breathing Behavior and Pore Surface in Zr□MOFs by Reversible Post□Synthetic Variable□Spacer Installation to Fine□Tune the Expansion Magnitude and Sorption Properties. *Angew. Chem., Int. Ed.* **2016,** *55* (34), 9932-9936.

69. Yang, Q.; Wiersum, A. D.; Llewellyn, P. L.; Guillerm, V.; Serred, C.; Maurin, G., Functionalizing porous zirconium terephthalate UiO-66(Zr) for natural gas upgrading: a computational exploration. *Chem. Commun.* **2011,** *47* (34), 9603-9605.

70. Yang, Q.; Guillerm, V.; Ragon, F.; Wiersum, A. D.; Llewellyn, P. L.; Zhong, C.; Devic, T.; Serre, C.; Maurin, G., CH_4 storage and CO_2 capture in highly porous zirconium oxide based metal-organic frameworks. *Chem. Commun.* **2012,** *48* (79), 9831-9833.

71. Gutov, O. V.; Molina, S.; Escudero□Adán, E. C.; Shafir, A., Modulation by Amino Acids: Toward Superior Control in the Synthesis of Zirconium Metal–Organic Frameworks. *Chem. Eur. J.* **2016,** *22* (38), 13582-13587.

72. Marshall, R. J.; Hobday, C. L.; Murphie, C. F.; Griffin, S. L.; Morrison, C. A.; Moggach, S. A.; Forgan, R. S., Amino acids as highly efficient modulators for single crystals of zirconium and hafnium metal-organic frameworks. *J. Mater. Chem. A* **2016,** *4* (18), 6955-6963.

73. Lü, B.; Chen, Y.; Li, P.; Wang, B.; Müllen, K.; Yin, M., Stable radical anions generated from a porous perylenediimide metal-organic framework for boosting near-infrared photothermal conversion. *Nat. Commun.* **2019,** *10* (1), 767.

74. Eddaoudi, M.; Kim, J.; Wachter, J. B.; Chae, H. K.; O'Keeffe, M.; Yaghi, O. M., Porous metal-organic polyhedra: 25 angstrom cuboctahedron constructed from 12 $Cu_2(CO_2)_4$ paddle-wheel building blocks. *J. Am. Chem. Soc.* **2001,** *123* (18), 4368-4369.

75. Abourahma, H.; Coleman, A. W.; Moulton, B.; Rather, B.; Shahgaldian, P.; Zaworotko, M. J., Hydroxylated nanoballs: synthesis, crystal structure, solubility and crystallization on surfaces. *Chem. Commun.* **2001,** (22), 2380-2381.

76. Perry, J. J. I.; Perman, J. A.; Zaworotko, M. J., Design and synthesis of metal-organic frameworks using metal-organic polyhedra as supermolecular building blocks. *Chem. Soc. Rev.* **2009,** *38* (5), 1400-1417.

77. Chakrabarty, R.; Mukherjee, P. S.; Stang, P. J., Supramolecular Coordination: Self-Assembly of Finite Two- and Three-Dimensional Ensembles. *Chem. Rev.* **2011,** *111* (11), 6810-6918.

78. Cook, T. R.; Zheng, Y.-R.; Stang, P. J., Metal–Organic Frameworks and Self-Assembled Supramolecular Coordination Complexes: Comparing and Contrasting the Design, Synthesis, and Functionality of Metal–Organic Materials. *Chem. Rev.* **2013,** *113* (1), 734-777.

79. Tranchemontagne, D. J.; Ni, Z.; O'Keeffe, M.; Yaghi, O. M., Reticular Chemistry of Metal–Organic Polyhedra. *Angew. Chem., Int. Ed.* **2008,** *47* (28), 5136-5147.

80. Li, J.-R.; Yakovenko, A. A.; Lu, W.; Timmons, D. J.; Zhuang, W.; Yuan, D.; Zhou, H.-C., Ligand Bridging-Angle-Driven Assembly of Molecular Architectures Based on Quadruply Bonded Mo-Mo Dimers. *J. Am. Chem. Soc.* **2010,** *132* (49), 17599-17610.

81. Fujita, D.; Ueda, Y.; Sato, S.; Mizuno, N.; Kumasaka, T.; Fujita, M., Self-assembly of tetravalent Goldberg polyhedra from 144 small components. *Nature* **2016,** *540*, 563.

82. Wang, B.; Huang, H.; Lv, X.-L.; Xie, Y.; Li, M.; Li, J.-R., Tuning CO_2 Selective Adsorption over N_2 and CH_4 in UiO-67 Analogues through Ligand Functionalization. *Inorg. Chem.* **2014,** *53* (17), 9254-9259.

83. Bon, V.; Senkovskyy, V.; Senkovska, I.; Kaskel, S., Zr(iv) and Hf(iv) based metal-organic frameworks with reo-topology. *Chem. Commun.* **2012,** *48* (67), 8407-8409.

84. Sun, X.; Gu, J.; Yuan, Y.; Yu, C.; Li, J.; Shan, H.; Li, G.; Liu, Y., A Stable Mesoporous Zr-Based Metal Organic Framework for Highly Efficient CO2 Conversion. *Inorg. Chem.* **2019,** *58* (11), 7480-7487.

85. Bon, V.; Senkovska, I.; Baburin, I. A.; Kaskel, S., Zr- and Hf-Based Metal–Organic Frameworks: Tracking Down the Polymorphism. *Cryst. Growth Des.* **2013,** *13* (3), 1231-1237.

86. Drache, F.; Bon, V.; Senkovska, I.; Getzschmann, J.; Kaskel, S., The modulator driven polymorphism of Zr(IV) based metal–organic frameworks. *Phil. Trans. R. Soc. A* **2017,** *375*, 20160027.

87. Dreischarf, A. C.; Lammert, M.; Stock, N.; Reinsch, H., Green Synthesis of Zr-CAU-28: Structure and Properties of the First Zr-MOF Based on 2,5-Furandicarboxylic Acid. *Inorg. Chem.* **2017,** *56* (4), 2270-2277.

88. Xie, L.-H.; Liu, X.-M.; He, T.; Li, J.-R., Metal-Organic Frameworks for the Capture of Trace Aromatic Volatile Organic Compounds. *Chem* **2018,** *4* (8), 1911-1927.

89. Wei, W.; Wang, X.; Zhang, K.; Tian, C.-B.; Du, S.-W., Tuning the Topology from fcu to pcu: Synthesis and Magnetocaloric Effect of Metal–Organic Frameworks Based on a Hexanuclear Gd(III)-Hydroxy Cluster. *Cryst. Growth Des.* **2019,** *19* (1), 55-59.

90. Krause, S.; Bon, V.; Stoeck, U.; Senkovska, I.; Többens, D. M.; Wallacher, D.; Kaskel, S., A Stimuli-Responsive Zirconium Metal–Organic Framework Based on Supermolecular Design. *Angew. Chem., Int. Ed.* **2017,** *56* (36), 10676-10680.

91. Szuromi, P., Transversal zigzag linkers. *Science* **2018,** *361* (6405), 889-890.

92. Chen, Z.-F.; Zhang, Z.-L.; Tan, Y.-H.; Tang, Y.-Z.; Fun, H.-K.; Zhou, Z.-Y.; Abrahams, B. F.; Liang, H., Coordination polymers constructed by linking metal ions with azodibenzoate anions. *CrystEngComm* **2008,** *10* (2), 217-231.

93. Wang, X.-S.; Ma, S.; Rauch, K.; Simmons, J. M.; Yuan, D.; Wang, X.; Yildirim, T.; Cole, W. C.; Lopez, J. J.; de Meijere, A.; Zhou, H.-C., Metal-organic frameworks based on double-bond-coupled di-isophthalate linkers with high hydrogen and methane uptakes. *Chem. Mater.* **2008,** *20* (9), 3145-3152.

94. Kim, H.-C.; Huh, S.; Kim, S.-J.; Kim, Y., Selective carbon dioxide sorption and heterogeneous catalysis by a new 3D Zn-MOF with nitrogen-rich 1D channels. *Sci. Rep.* **2017,** *7* (1), 17185.

95. Wahiduzzaman, M.; Wang, S.; Sikora, B. J.; Serre, C.; Maurin, G., Computational structure determination of novel metal–organic frameworks. *Chem. Commun.* **2018,** *54* (77), 10812-10815.

96. Nguyen, H. T. T.; Tu, T. N.; Nguyen, M. V.; Lo, T. H. N.; Furukawa, H.; Nguyen, N. N.; Nguyen, M. D., Combining Linker Design and Linker-Exchange Strategies for the Synthesis of a Stable Large-Pore Zr-Based Metal–Organic Framework. *ACS Appl. Mater. Interfaces* **2018,** *10* (41), 35462-35468.

97. Guillerm, V.; Ragon, F.; Dan-Hardi, M.; Devic, T.; Vishnuvarthan, M.; Campo, B.; Vimont, A.; Clet, G.; Yang, Q.; Maurin, G.; Férey, G.; Vittadini, A.; Gross, S.; Serre, C., A series of isoreticular, highly stable, porous zirconium oxide based metal-organic frameworks. *Angew. Chem., Int. Ed.* **2012,** *51* (37), 9267-71.

98. Guillerm, V.; Xu, H.; Albalad, J.; Imaz, I.; Maspoch, D., Post-Synthetic Selective Ligand Cleavage by Solid-Gas Phase Ozonolysis Fuses Micropores into Mesopores in Metal-Organic Frameworks. *J. Am. Chem. Soc.* **2018,** *140* (44), 15022-15030.

99. Yuan, S.; Zou, L.; Qin, J.-S.; Li, J.; Huang, L.; Feng, L.; Wang, X.; Bosch, M.; Alsalme, A.; Cagin, T.; Zhou, H.-C., Construction of hierarchically porous metal–organic frameworks through linker labilization. *Nat. Commun.* **2017,** *8*, 15356.

100. Chevreau, H.; Devic, T.; Salles, F.; Maurin, G.; Stock, N.; Serre, C., Mixed-Linker Hybrid Superpolyhedra for the Production of a Series of Large-Pore Iron(III) Carboxylate Metal-Organic Frameworks. *Angew. Chem., Int. Ed.* **2013,** *52* (19), 5056-5060.

101. Bunck, D. N.; Dichtel, W. R., Mixed Linker Strategies for Organic Framework Functionalization. *Chem. Eur. J.* **2013,** *19* (3), 818-827.

102. Nelson, A. P.; Parrish, D. A.; Cambrea, L. R.; Baldwin, L. C.; Trivedi, N. J.; Mulfort, K. L.; Farha, O. K.; Hupp, J. T., Crystal to Crystal Guest Exchange in a Mixed Ligand Metal−Organic Framework. *Cryst. Growth Des.* **2009,** *9* (11), 4588-4591.

103. Li, J.; Peng, Y.; Liang, H.; Yu, Y.; Xin, B.; Li, G.; Shi, Z.; Feng, S., Solvothermal Synthesis and Structural Characterisation of Metal-Organic Frameworks with Paddle-Wheel Zinc Carboxylate Clusters and Mixed Ligands. *Eur. J. Inorg. Chem.* **2011,** *2011* (17), 2712-2719.

104. Deng, H.; Doonan, C. J.; Furukawa, H.; Ferreira, R. B.; Towne, J.; Knobler, C. B.; Wang, B.; Yaghi, O. M., Multiple Functional Groups of Varying Ratios in Metal-Organic Frameworks. *Science* **2010,** *327* (5967), 846-850.

105. Koh, K.; Wong-Foy, A. G.; Matzger, A. J., A Crystalline Mesoporous Coordination Copolymer with High Microporosity. *Angew. Chem., Int. Ed.* **2008,** *47* (4), 677-680.

106. Koh, K.; Wong-Foy, A. G.; Matzger, A. J., A Porous Coordination Copolymer with over 5000 m^2/g BET Surface Area. *J. Am. Chem. Soc.* **2009,** *131* (12), 4184-4185.

107. Zhai, Q.-G.; Bu, X.; Zhao, X.; Li, D.-S.; Feng, P., Pore Space Partition in Metal–Organic Frameworks. *Acc. Chem. Res.* **2017,** *50* (2), 407-417.

108. Liu, L.; Konstas, K.; Hill, M. R.; Telfer, S. G., Programmed Pore Architectures in Modular Quaternary Metal–Organic Frameworks. *J. Am. Chem. Soc.* **2013,** *135* (47), 17731-17734.

109. Kim, H.; Kim, D.; Moon, D.; Choi, Y. N.; Baek, S. B.; Lah, M. S., Symmetry-guided syntheses of mixed-linker Zr metal-organic frameworks with precise linker locations. *Chem. Sci.* **2019,** *10* (22), 5801-5806.

110. Nguyen, T. T. M.; Le, H. M.; Kawazoe, Y.; Nguyen, H. L., Reticular control of interpenetration in a complex metal–organic framework. *Mater. Chem. Front.* **2018,** *2* (11), 2063-2069.

111. He, T.; Zhang, Y.-Z.; Kong, X.-J.; Yu, J.; Lv, X.-L.; Wu, Y.; Guo, Z.-J.; Li, J.-R., Zr(IV)-Based Metal-Organic Framework with T-Shaped Ligand: Unique Structure, High Stability, Selective Detection, and Rapid Adsorption of Cr2O72– in Water. *ACS Appl. Mater. Interfaces* **2018,** *10* (19), 16650-16659.

112. Kickelbick, G.; Schubert, U., Oxozirconium Methacrylate Clusters: $Zr_6(OH)_4O_4(OMc)_{12}$ and $Zr_4O_2(OMc)_{12}$ (OMc = Methacrylate). *Chem. Ber.* **1997,** *130* (4), 473-478.

113. Otero, A.; Fernández-Baeza, J.; Antiñolo, A.; Tejeda, J.; Lara-Sánchez, A.; Sánchez-Barba, L.; Fernández-López, M.; López-Solera, I., New Complexes of Zirconium(IV) and Hafnium(IV) with Heteroscorpionate Ligands and the Hydrolysis of Such Complexes To Give a Zirconium Cluster. *Inorg. Chem.* **2004,** *43* (4), 1350-1358.

114. Schaate, A.; Roy, P.; Godt, A.; Lippke, J.; Waltz, F.; Wiebcke, M.; Behrens, P., Modulated Synthesis of Zr□Based Metal–Organic Frameworks: From Nano to Single Crystals. *Chem. Eur. J.* **2011,** *17* (24), 6643-6651.

115. Coudert, F.-X. https://twitter.com/MOF_papers/status/1071974578400845824

116. Chen, Z.; Hanna, S. L.; Redfern, L. R.; Alezi, D.; Islamoglu, T.; Farha, O. K., Reticular chemistry in the rational synthesis of functional zirconium cluster-based MOFs. *Coord. Chem. Rev.* **2019,** *386*, 32-49.

117. Bai, Y.; Dou, Y.; Xie, L.-H.; Rutledge, W.; Li, J.-R.; Zhou, H.-C., Zr-based metal–organic frameworks: design, synthesis, structure, and applications. *Chem. Soc. Rev.* **2016,** *45* (8), 2327-2367.

118. Feng, D.; Wang, K.; Su, J.; Liu, T.-F.; Park, J.; Wei, Z.; Bosch, M.; Yakovenko, A.; Zou, X.; Zhou, H.-C., A Highly Stable Zeotype Mesoporous Zirconium Metal–Organic Framework with Ultralarge Pores. *Angew. Chem., Int. Ed.* **2015,** *54* (1), 149-154.

119. Wang, R.; Wang, Z.; Xu, Y.; Dai, F.; Zhang, L.; Sun, D., Porous Zirconium Metal–Organic Framework Constructed from 2D → 3D Interpenetration Based on a 3,6-Connected kgd Net. *Inorg. Chem.* **2014,** *53* (14), 7086-7088.

120. Wang, B.; Lv, X.-L.; Feng, D.; Xie, L.-H.; Zhang, J.; Li, M.; Xie, Y.; Li, J.-R.; Zhou, H.-C., Highly Stable Zr(IV)-Based Metal–Organic Frameworks for the Detection and Removal of Antibiotics and Organic Explosives in Water. *J. Am. Chem. Soc.* **2016,** *138* (19), 6204-6216.

121. Lee, S.; Bürgi, H.-B.; Alshmimri, S. A.; Yaghi, O. M., Impact of Disordered Guest–Framework Interactions on the Crystallography of Metal–Organic Frameworks. *J. Am. Chem. Soc.* **2018,** *140* (28), 8958-8964.

122. Guo, B.; Li, F.; Wang, C.; Zhang, L.; Sun, D., A rare (3,12)-connected zirconium metal–organic framework with efficient iodine adsorption capacity and pH sensing. *J. Mater. Chem. A* **2019,** *7* (21), 13173-13179.

123. Furukawa, H.; Go, Y. B.; Ko, N.; Park, Y. K.; Uribe-Romo, F. J.; Kim, J.; O'Keeffe, M.; Yaghi, O. M., Isoreticular Expansion of Metal-Organic Frameworks with Triangular and Square Building Units and the Lowest Calculated Density for Porous Crystals. *Inorg. Chem.* **2011,** *50* (18), 9147-9152.

124. Sun, D.; Ma, S.; Ke, Y.; Collins, D. J.; Zhou, H.-C., An Interweaving MOF with High Hydrogen Uptake. *J. Am. Chem. Soc.* **2006,** *128* (12), 3896-3897.

125. Wong-Foy, A. G.; Lebel, O.; Matzger, A. J., Porous crystal derived from a tricarboxylate linker with two distinct binding motifs. *J. Am. Chem. Soc.* **2007,** *129* (51), 15740-15741.

126. Lim, C.-S.; Schnobrich, J. K.; Wong-Foy, A. G.; Matzger, A. J., Metal-Dependent Phase Selection in Coordination Polymers Derived from a C_{2v}-Symmetric Tricarboxylate. *Inorg. Chem.* **2010,** *49* (11), 5271-5275.

127. Lu, Z.; Du, L.; Zheng, B.; Bai, J.; Zhang, M.; Yun, R., A highly porous agw-type metal–organic framework and its CO2 and H2 adsorption capacity. *CrystEngComm* **2013,** *15* (45), 9348-9351.

128. Schnobrich, J. K.; Lebel, O.; Cychosz, K. A.; Dailly, A.; Wong-Foy, A. G.; Matzger, A. J., Linker-Directed Vertex Desymmetrization for the Production of Coordination Polymers with High Porosity. *J. Am. Chem. Soc.* **2010,** *132* (39), 13941-13948.

129. Stoeck, U.; Senkovska, I.; Bon, V.; Krause, S.; Kaskel, S., Assembly of metal–organic polyhedra into highly porous frameworks for ethene delivery. *Chem. Commun.* **2015,** *51* (6), 1046-1049.

130. Li, J.-R.; Timmons, D. J.; Zhou, H.-C., Interconversion between Molecular Polyhedra and Metal-Organic Frameworks. *J. Am. Chem. Soc.* **2009,** *131* (18), 6368-6369.

131. Mellot-Draznieks, C.; Dutour, J.; Férey, G., Computational design of hybrid frameworks: Structure and energetics of two $Me_3OF_3\{^-O_2C\text{-}C_6H_4\text{-}CO_2^-\}_3$ metal-dicarboxylate polymorphs, MIL-hypo-1 and MIL-hypo-2. *Z. Anorg. Allg. Chem.* **2004,** *630* (15), 2599-2604.

132. Mellot-Draznieks, C.; Dutour, J.; Férey, G., Hybrid Organic–Inorganic Frameworks: Routes for Computational Design and Structure Prediction. *Angew. Chem.* **2004,** *116* (46), 6450-6456.

133. Horcajada, P.; Chevreau, H.; Heurtaux, D.; Benyettou, F.; Salles, F.; Devic, T.; Garcia-Marquez, A.; Yu, C.; Lavrard, H.; Dutson, C. L.; Magnier, E.; Maurin, G.; Elkaïm, E.; Serre, C., Extended and functionalized porous iron(iii) tri- or dicarboxylates with MIL-100/101 topologies. *Chem. Commun.* **2014,** *50* (52), 6872-6874.

134. Feng, D.; Liu, T.-F.; Su, J.; Bosch, M.; Wei, Z.; Wan, W.; Yuan, D.; Chen, Y.-P.; Wang, X.; Wang, K.; Lian, X.; Gu, Z.-Y.; Park, J.; Zou, X.; Zhou, H.-C., Stable metal-organic frameworks containing single-molecule traps for enzyme encapsulation. *Nat. Commun.* **2015,** *6*, 5979.

135. Lian, X.; Chen, Y.-P.; Liu, T.-F.; Zhou, H.-C., Coupling two enzymes into a tandem nanoreactor utilizing a hierarchically structured MOF. *Chem. Sci.* **2016,** *7* (12), 6969-6973.

136. Ibarra, I. A.; Lin, X.; Yang, S.; Blake, A. J.; Walker, G. S.; Barnett, S. A.; Allan, D. R.; Champness, N. R.; Hubberstey, P.; Schröder, M., Structures and H_2 Adsorption Properties of Porous Scandium Metal–Organic Frameworks. *Chem. Eur. J.* **2010,** *16* (46), 13671-13679.

137. 3,6T60 code. https://topcryst.com/ (accessed 29-jul-19).

138. Chae, H. K.; Siberio-Perez, D. Y.; Kim, J.; Go, Y.; Eddaoudi, M.; Matzger, A. J.; O'Keeffe, M.; Yaghi, O. M., A route to high surface area, porosity and inclusion of large molecules in crystals. *Nature* **2004,** *427* (6974), 523-527.

139. 3,3,3,6,6T17 code. https://topcryst.com/ (accessed 29-jul-19).

140. 3,3,6T51 code. https://topcryst.com/ (accessed 29-jul-19).

141. Feng, D.; Wang, K.; Wei, Z.; Chen, Y.-P.; Simon, C. M.; Arvapally, R. K.; Martin, R. L.; Bosch, M.; Liu, T.-F.; Fordham, S.; Yuan, D.; Omary, M. A.; Haranczyk, M.; Smit, B.; Zhou, H.-C., Kinetically tuned dimensional augmentation as a versatile synthetic route towards robust metal–organic frameworks. *Nat. Commun.* **2014,** *5*, 5723.

142. Zhang, J.-W.; Ji, W.-J.; Hu, M.-C.; Li, S.-N.; Jiang, Y.-C.; Zhang, X.-M.; Qu, P.; Zhai, Q.-G., A superstable 3p-block metal–organic framework platform towards prominent CO_2 and C_1/C_2-hydrocarbon uptake and separation performance and strong Lewis acid catalysis for CO_2 fixation. *Inorg. Chem. Front.* **2019,** *6* (3), 813-819.

143. Zhang, F.-M.; Dong, L.-Z.; Qin, J.-S.; Guan, W.; Liu, J.; Li, S.-L.; Lu, M.; Lan, Y.-Q.; Su, Z.-M.; Zhou, H.-C., Effect of Imidazole Arrangements on Proton-Conductivity in Metal–Organic Frameworks. *J. Am. Chem. Soc.* **2017,** *139* (17), 6183-6189.

144. Chae, H. K.; Kim, J.; Friedrichs, O. D.; O'Keeffe, M.; Yaghi, O. M., Design of Frameworks with Mixed Triangular and Octahedral Building Blocks Exemplified by the Structure of $[Zn_4O(TCA)_2]$ Having the Pyrite Topology. *Angew. Chem., Int. Ed.* **2003,** *42* (33), 3907-3909.

145. Zhang, Y.-B.; Furukawa, H.; Ko, N.; Nie, W.; Park, H. J.; Okajima, S.; Cordova, K. E.; Deng, H.; Kim, J.; Yaghi, O. M., Introduction of Functionality, Selection of Topology, and Enhancement of Gas Adsorption in Multivariate Metal–Organic Framework-177. *J. Am. Chem. Soc.* **2015,** *137* (7), 2641-2650.

146. Jiang, J.; Furukawa, H.; Zhang, Y.-B.; Yaghi, O. M., High Methane Storage Working Capacity in Metal–Organic Frameworks with Acrylate Links. *J. Am. Chem. Soc.* **2016,** *138* (32), 10244-10251.

147. Furukawa, H.; Ko, N.; Go, Y. B.; Aratani, N.; Choi, S. B.; Choi, E.; Yazaydin, A. Ö.; Snurr, R. Q.; O'Keeffe, M.; Kim, J.; Yaghi, O. M., Ultrahigh Porosity in Metal-Organic Frameworks. *Science* **2010,** *329* (5990), 424-428.

148. Verma, A.; De, D.; Tomar, K.; Bharadwaj, P. K., An Amine Functionalized Metal–Organic Framework as an Effective Catalyst for Conversion of CO_2 and Biginelli Reactions. *Inorg. Chem.* **2017,** *56* (16), 9765-9771.

149. Fan, W.; Wang, Y.; Xiao, Z.; Zhang, L.; Gong, Y.; Dai, F.; Wang, R.; Sun, D., A Stable Amino-Functionalized Interpenetrated Metal–Organic Framework Exhibiting Gas Selectivity and Pore-Size-Dependent Catalytic Performance. *Inorg. Chem.* **2017,** *56* (22), 13634-13637.

150. Kong, L.; Zou, R.; Bi, W.; Zhong, R.; Mu, W.; Liu, J.; Han, R. P. S.; Zou, R., Selective adsorption of CO_2/CH_4 and CO_2/N_2 within a charged metal–organic framework. *J. Mater. Chem. A* **2014,** *2* (42), 17771-17778.

151. Chen, B. L.; Ockwig, N. W.; Millward, A. R.; Contreras, D. S.; Yaghi, O. M., High H-2 adsorption in a microporous metal-organic framework with open metal sites. *Angew. Chem., Int. Ed.* **2005,** *44* (30), 4745-4749.

152. He, Y.; Li, B.; O'Keeffe, M.; Chen, B., Multifunctional metal-organic frameworks constructed from meta-benzenedicarboxylate units. *Chem. Soc. Rev.* **2014,** *43* (16), 5618-5656.

153. Lu, W.; Wei, Z.; Gu, Z.-Y.; Liu, T.-F.; Park, J.; Park, J.; Tian, J.; Zhang, M.; Zhang, Q.; Gentle III, T.; Bosch, M.; Zhou, H.-C., Tuning the structure and function of metal-organic frameworks via linker design. *Chem. Soc. Rev.* **2014,** *43* (16), 5561-93.

154. Wang, X.-S.; Ma, S.; Forster, P. M.; Yuan, D.; Eckert, J.; López, J. J.; Murphy, B. J.; Parise, J. B.; Zhou, H.-C., Enhancing H_2 Uptake by "Close-Packing" Alignment of Open Copper Sites in Metal–Organic Frameworks. *Angew. Chem., Int. Ed.* **2008,** *47* (38), 7263-7266.

155. Duan, X.; Yu, J.; Cai, J.; He, Y.; Wu, C.; Zhou, W.; Yildirim, T.; Zhang, Z.; Xiang, S.; O'Keeffe, M.; Chen, B.; Qian, G., A microporous metal-organic framework of a rare sty topology for high CH_4 storage at room temperature. *Chem. Commun.* **2013,** *49* (20), 2043-2045.

156. Lin, X.; Telepeni, I.; Blake, A. J.; Dailly, A.; Brown, C. M.; Simmons, J. M.; Zoppi, M.; Walker, G. S.; Thomas, K. M.; Mays, T. J.; Hubberstey, P.; Champness, N. R.; Schroeder, M., High Capacity Hydrogen Adsorption in Cu(II) Tetracarboxylate Framework Materials: The Role of Pore Size, Ligand Functionalization, and Exposed Metal Sites. *J. Am. Chem. Soc.* **2009,** *131* (6), 2159-2171.

157. Grünker, R.; Senkovska, I.; Biedermann, R.; Klein, N.; Klausch, A.; Baburin, I. A.; Mueller, U.; Kaskel, S., Topological Diversity, Adsorption and Fluorescence Properties of MOFs Based on a Tetracarboxylate Ligand. *Eur. J. Inorg. Chem.* **2010,** *2010* (24), 3835-3841.

158. Sun, D.; Ke, Y.; Mattox, T. M.; Ooro, B. A.; Zhou, H.-C., Temperature-dependent supramolecular stereoisomerism in porous copper coordination networks based on a designed carboxylate ligand. *Chem. Commun.* **2005,** (43), 5447-5449.

159. Sun, D.; Collins, D. J.; Ke, Y.; Zuo, J.-L.; Zhou, H.-C., Construction of open metal-organic frameworks based on predesigned carboxylate isomers: From achiral to chiral nets. *Chem. Eur. J.* **2006,** *12* (14), 3768-3776.

160. Lu, W.; Yuan, D.; Makal, T. A.; Wei, Z.; Li, J.-R.; Zhou, H.-C., Highly porous metal-organic framework sustained with 12-connected nanoscopic octahedra. *Dalton Trans.* **2013,** *42* (5), 1708-1714.

161. Krause, S.; Bon, V.; Senkovska, I.; Stoeck, U.; Wallacher, D.; Többens, D. M.; Zander, S.; Pillai, R. S.; Maurin, G.; Coudert, F.-X.; Kaskel, S., A pressure-amplifying framework material with negative gas adsorption transitions. *Nature* **2016,** *532*, 348.

162. Feng, D.; Chung, W.-C.; Wei, Z.; Gu, Z.-Y.; Jiang, H.-L.; Chen, Y.-P.; Darensbourg, D. J.; Zhou, H.-C., Construction of Ultrastable Porphyrin Zr Metal–Organic Frameworks through Linker Elimination. *J. Am. Chem. Soc.* **2013,** *135* (45), 17105-17110.

163. Kung, C.-W.; Wang, T. C.; Mondloch, J. E.; Fairen-Jimenez, D.; Gardner, D. M.; Bury, W.; Klingsporn, J. M.; Barnes, J. C.; Van Duyne, R.; Stoddart, J. F.; Wasielewski, M. R.; Farha, O. K.; Hupp, J. T., Metal–Organic Framework Thin Films Composed of Free-Standing Acicular Nanorods Exhibiting Reversible Electrochromism. *Chem. Mater.* **2013,** *25* (24), 5012-5017.

164. Feng, D.; Gu, Z.-Y.; Chen, Y.-P.; Park, J.; Wei, Z.; Sun, Y.; Bosch, M.; Yuan, S.; Zhou, H.-C., A Highly Stable Porphyrinic Zirconium Metal–Organic Framework with shp-a Topology. *J. Am. Chem. Soc.* **2014,** *136* (51), 17714-17717.

165. Jiang, H.-L.; Feng, D.; Wang, K.; Gu, Z.-Y.; Wei, Z.; Chen, Y.-P.; Zhou, H.-C., An Exceptionally Stable, Porphyrinic Zr Metal–Organic Framework Exhibiting pH-Dependent Fluorescence. *J. Am. Chem. Soc.* **2013,** *135* (37), 13934-13938.

166. Nguyen, P. T. K.; Nguyen, H. T. D.; Nguyen, H. N.; Trickett, C. A.; Ton, Q. T.; Gutiérrez-Puebla, E.; Monge, M. A.; Cordova, K. E.; Gándara, F., New Metal–Organic Frameworks for Chemical Fixation of CO_2. *ACS Appl. Mater. Interfaces* **2018,** *10* (1), 733-744.

167. Wang, H.; Dong, X.; Lin, J.; Teat, S. J.; Jensen, S.; Cure, J.; Alexandrov, E. V.; Xia, Q.; Tan, K.; Wang, Q.; Olson, D. H.; Proserpio, D. M.; Chabal, Y. J.; Thonhauser, T.; Sun, J.; Han, Y.; Li, J., Topologically guided tuning of Zr-MOF pore structures for highly selective separation of C_6 alkane isomers. *Nat. Commun.* **2018,** *9* (1), 1745.

168. Luebke, R.; Belmabkhout, Y.; Weseliński, Ł. J.; Cairns, A. J.; Alkordi, M.; Norton, G.; Wojtas, Ł.; Adil, K.; Eddaoudi, M., Versatile rare earth hexanuclear clusters for the design and synthesis of highly-connected ftw-MOFs. *Chem. Sci.* **2015,** *6* (7), 4095-4102.

169. 3,3,8T132 code. https://topcryst.com/ (accessed 29-jul-19).

170. Pang, J.; Yuan, S.; Qin, J.; Liu, C.; Lollar, C.; Wu, M.; Yuan, D.; Zhou, H.-C.; Hong, M., Control the Structure of Zr-Tetracarboxylate Frameworks through Steric Tuning. *J. Am. Chem. Soc.* **2017,** *139* (46), 16939-16945.

171. Lammert, M.; Reinsch, H.; Murray, C. A.; Wharmby, M. T.; Terraschke, H.; Stock, N., Synthesis and structure of Zr(iv)- and Ce(iv)-based CAU-24 with 1,2,4,5-tetrakis(4-carboxyphenyl)benzene. *Dalton Trans.* **2016,** *45* (47), 18822-18826.

172. Lyu, J.; Zhang, X.; Otake, K.-i.; Wang, X.; Li, P.; Li, Z.; Chen, Z.; Zhang, Y.; Wasson, M. C.; Yang, Y.; Bai, P.; Guo, X.; Islamoglu, T.; Farha, O. K., Topology and porosity control of metal–organic frameworks through linker functionalization. *Chem. Sci.* **2019,** *10* (4), 1186-1192.

173. Zou, Y.; Park, M.; Hong, S.; Lah, M. S., A designed metal-organic framework based on a metal-organic polyhedron. *Chem. Commun.* **2008,** (20), 2340-2342.

174. Luebke, R.; Eubank, J. F.; Cairns, A. J.; Belmabkhout, Y.; Wojtas, Ł.; Eddaoudi, M., The unique rht-MOF platform, ideal for pinpointing the functionalization and CO_2 adsorption relationship. *Chem. Commun.* **2012,** *48* (10), 1455-1457.

175. Farha, O. K.; Eryazici, I.; Jeong, N. C.; Hauser, B. G.; Wilmer, C. E.; Sarjeant, A. A.; Snurr, R. Q.; Nguyen, S. T.; Yazaydın, A. Ö.; Hupp, J. T., Metal–Organic Framework Materials with Ultrahigh Surface Areas: Is the Sky the Limit? *J. Am. Chem. Soc.* **2012,** *134* (36), 15016-15021.

176. Zhao, D.; Yuan, D.; Sun, D.; Zhou, H.-C., Stabilization of Metal-Organic Frameworks with High Surface Areas by the Incorporation of Mesocavities with Microwindows. *J. Am. Chem. Soc.* **2009,** *131* (26), 9186-9187.

177. Guo, Z.; Wu, H.; Srinivas, G.; Zhou, Y.; Xiang, S.; Chen, Z.; Yang, Y.; Zhou, W.; O'Keeffe, M.; Chen, B., A Metal-Organic Framework with Optimized Open Metal Sites and Pore Spaces for High Methane Storage at Room Temperature. *Angew. Chem., Int. Ed.* **2011,** *50* (14), 3178-3181.

178. Li, J.-R.; Zhou, H.-C., Metal-Organic Hendecahedra Assembled from Dinuclear Paddlewheel Nodes and Mixtures of Ditopic Linkers with 120 and 90 degrees Bend Angles. *Angew. Chem., Int. Ed.* **2009,** *48* (45), 8465-8468.